ANL/RERTR/TM-07-01

Argonne NATIONAL LABORATORY

Fundamental Approach to TRIGA Steady-State Thermal-Hydraulic CHF Analysis

Nuclear Engineering Division

About Argonne National Laboratory

Argonne is a U.S. Department of Energy laboratory managed by UChicago Argonne, LLC under contract DE-AC02-06CH11357. The Laboratory's main facility is outside Chicago, at 9700 South Cass Avenue, Argonne, Illinois 60439. For information about Argonne, see www.anl.gov.

Availability of This Report

This report is available, at no cost, at http://www.osti.gov/bridge. It is also available on paper to the U.S. Department of Energy and its contractors, for a processing fee, from:

U.S. Department of Energy
Office of Scientific and Technical Information
P.O. Box 62
Oak Ridge, TN 37831-0062
phone (865) 576-8401
fax (865) 576-5728
reports@adonis.osti.gov

ANL/RERTR/TM-07-01

Fundamental Approach to TRIGA Steady-State Thermal-Hydraulic CHF Analysis

by
E.E. Feldman
Nuclear Engineering Division, Argonne National Laboratory

December 2007

TABLE OF CONTENTS

LIST OF FIGURES

LIST OF TABLES

 ANL/RERTR/TM-07-01

FUNDAMENTAL APPROACH TO TRIGA STEADY-STATE THERMAL-HYDRAULIC CHF ANALYSIS

Earl E. Feldman

Reduced Enrichment for Research and Test Reactors Program
Nuclear Engineering Division
Argonne National Laboratory
9700 S. Cass Avenue
Argonne, Illinois 60439

ABSTRACT

Methods are investigated for predicting the power at which critical heat flux (CHF) occurs in TRIGA reactors that rely on natural convection for primary flow. For a representative TRIGA reactor, two sets of functions are created. For the first set, the General Atomics STAT code and the more widely-used RELAP5-3D code are each employed to obtain reactor flow rate as a function of power. For the second set, the Bernath correlation, the 2006 Groeneveld table, the Hall and Mudawar outlet correlation, and each of the four PG-CHF correlations for rod bundles are used to predict the power at which CHF occurs as a function of channel flow rate. The two sets of functions are combined to yield predictions of the power at which CHF occurs in the reactor. A combination of the RELAP5-3D code and the 2006 Groeneveld table predicts 67% more CHF power than does a combination of the STAT code and the Bernath correlation. Replacing the 2006 Groeneveld table with the Bernath CHF correlation (while using the RELAP5-3D code flow solution) causes the increase to be 23% instead of 67%. Additional RELAP5-3D flow-versus-power solutions obtained from Reference 1 and presented in Appendix B for four specific TRIGA reactors further demonstrates that the Bernath correlation predicts CHF to occur at considerably lower power levels than does the 2006 Groeneveld table. Because of the lack of measured CHF data in the region of interest to TRIGA reactors, none of the CHF correlations considered can be assumed to provide the definitive CHF power. It is recommended, however, to compare the power levels of the potential limiting rods with the power levels at which the Bernath and 2006 Groeneveld CHF correlations predict CHF to occur.

1 INTRODUCTION

TRIGA reactors that rely on natural convection for primary flow are among the most common research reactors in the US. Because during normal operation these reactors may operate with subcooled nucleate boiling, the margin to critical heat flux (CHF) can be a limiting design criterion. The purpose of this report is to provide insight into the thermal-hydraulic analysis and the prediction of CHF for TRIGA reactors that rely on natural convection for primary flow. This effort, which emphasizes CHF, has been coordinated with a similar parallel study[1] at General Atomics (GA) in San Diego, California.

TRIGA reactors use fuel rods, which are oriented vertically. Each fuel rod has uranium fuel in a zirconium-hydride matrix sealed inside a 0.020-inch thick Type 304 stainless steel tube, whose outer diameter is about 1.4 or 1.5 inches, depending on the reactor. Each reactor is located near the bottom of a deep pool of water. The primary flow is driven solely by natural convection. The heat generated by the rods causes the water inside the rod bundle to be hotter and, therefore, less dense, than that of the rest of the water in the pool. This density difference causes the water to circulate between the rod bundle and the rest of the pool.

This family of TRIGA reactors can be divided into three distinct groups, based on rod arrangement – hexagonal, circular, and rectangular. The reactors in the hexagonal group position all of the fuel rods on a uniform triangular pitch so that each rod can be considered to be at the center of a hexagonal cell. The circular TRIGAs are similar to the hexagonal ones except that the rods are arranged in concentric circles about the center position. This causes the pitch to be non-uniform. Also, some of the flow in the circular design may enter from the lateral sides of the lower inlet plenum rather than from the bottom. The rectangular-pitch reactors were originally operated as Material Test Reactors (MTRs) with the fuel in plates. Subsequently, each MTR assembly was replaced with an unshrouded TRIGA conversion assembly containing four TRIGA rods on a rectangular pitch.

TRIGA reactors use fuel with stainless steel cladding and were designed to operate with nucleate boiling. This cladding has a much higher melting point and is much less susceptible to boiling-induced corrosion than the aluminum cladding used in MTR reactors. During normal operation of TRIGA reactors, vapor bubbles form on some of the fuel rod surfaces while the mix-mean temperature of the adjacent coolant remains below the saturation temperature. Thus, there is some subcooled boiling, but no bulk boiling.

The local agitation of the coolant that is caused by the nucleate boiling greatly enhances the heat transfer from the clad surface to the coolant stream. This helps to limit fuel rod surface temperatures. When these boiling conditions exist, the clad surface temperature will typically be no more than about 20° C higher than the local coolant saturation temperature. This temperature differential depends only on the local coolant

pressure and local clad surface heat flux and does not depend on the local coolant flow rate.

When nucleate boiling occurs, bubbles of vapor that form on the surface of the clad are collapsed by the surrounding liquid and both liquid and vapor are in contact with the surface. If the bubbles coalesce and blanket the surface with vapor or the surface dries out, then a condition, referred to as "departure from nucleate boiling" (DNB) and sometimes called "burn-out", has occurred. The heat flux at which this occurs is called the "critical heat flux" (CHF). DNB greatly degrades the ability of the coolant to remove heat from the surface of the clad and can cause very high fuel temperatures, leading to fuel failure. Therefore, a safe margin to CHF must be maintained at all times. The local mixed-mean coolant temperature (or coolant quality, if the saturation temperature has been reached), the flow velocity, and the pressure all affect the heat flux at which CHF occurs.

Section 2 focuses on computer codes for predicting flow rate. Section 3 focuses on correlations for predicting CHF. In these two sections, flow rate and CHF predictions for a representative TRIGA reactor are made. Section 4 compares and discusses the diverse CHF predicts produced by various combinations of the flow rate and CHF correlations for the representative TRIGA reactor. Section 5 provides conclusions.

2 COOLANT FLOW RATE

The TRIGA rods are arranged in a tight open lattice with pitch-to-diameter ratios typically less than 1.2. There are no devices to encourage cross flow among adjacent channels. Therefore, a reasonable and conservative model is one in which each channel formed by the cusps of immediately adjacent rods is treated as an isolated channel. Figure 1 shows example a triangular coolant subchannel for a hexagonal-pitch TRIGA and a square-pitch subchannel for a TRIGA conversion reactor. This model is conservative because in the analysis the coolant in the subchannel with the hottest coolant is not cooled by exchanging coolant with it cooler neighbors or by conducting heat to other channels.

Since the primary flow is driven solely by natural convection and is not pumped or regulated, there is not a fixed amount of primary flow that must be distributed among all of the flow channels. In the modeling, the flow of each channel is independent of its neighbors and can be analyzed separately. Only the potentially hottest channels need be considered. Channel flow rates need only be sufficient to prevent CHF. If CHF is avoided, nucleate boiling causes the peak fuel temperatures to be essentially independent of local coolant flow rates and temperatures.

In the steady-state analysis of a single channel, if the channel flow rate is known, many other key thermal quantities can be easily deduced without the need for a sophisticated computer code. When the coolant inlet temperature to the channel and the axial power distribution along the channel are both known, all that is needed is an energy

balance to determine the mixed-mean coolant temperature and enthalpy at each axial level along the channel.

The determination of the flow rate in the limiting channel typically employs a computer code. These codes use coolant momentum equations in which the buoyancy forces are equated with the combination of the hydraulic resistance forces and the momentum flux (or acceleration) forces. The buoyancy forces are a result of the differences in coolant density. The fuel rods heat the adjacent coolant and cause it to be less dense than that of the coolant in the remainder of the reactor tank. The presence of vapor will also contribute to buoyancy. The hydraulic resistance has three components: an inlet resistance, an exit resistance, and friction along the vertical surfaces of the fuel rods. The inlet and outlet resistance, which are represented by "K-loss" factors, are difficult to calculate accurately, although bounding values can be estimated. The K-losses for TRIGA reactors are investigated in Reference 1.

Boiling considerably complicates the thermal-hydraulic analysis necessary to predict the channel flow. Any boiling, even subcooled boiling, greatly increases the frictional resistance to coolant flow along the vertical surfaces of the fuel rods. Increased boiling increases vapor-induced voids. These produce greater buoyancy with which to drive flow. Thus, boiling produces opposing effects that can either increase or decrease flow. In a boiling channel the vapor and the liquid need not move at the same speed. Thus, boiling is a complex phenomenon for which current modeling methods heavily rely on empirical correlations.

Measurements have been made by GA in the recently converted (from HEU to LEU fuel) TRIGA reactor at Texas A & M University in which the inlet and outlet coolant temperatures of individual channels were measured and channel flow rates were inferred. These are discussed in the parallel GA study.[1] Oregon State University has made temperature measurements in individual coolant channels in their circular pitch TRIGA reactor. Both sets of test results can be used to validate analytical models that predict channel flow. One of the inherent limitations of this type of testing is that it is limited to normal operating powers, which are expected to produce flows that are considerably less than those produced at CHF conditions.

2.1 The STAT Code[2]

STAT is a GA proprietary code that was developed specifically for the steady-state analysis of a single coolant channel of a TRIGA reactor. The code predicts the channel flow rate, the bulk coolant temperatures, the heat fluxes and the CHF for the fuel rod surfaces. The channel can be formed in the cusps of adjacent fuel rods or can be a region of fluid surrounding a fuel rod. The code includes the effects of subcooled boiling.

The program was written by John F. Petersen at GA Technologies and is, at least in part, based on Reference 3. As is a common and appropriate practice in this type of modeling, the coolant channel is divided into a series of horizontal layers and solved one

layer at a time, starting at the channel inlet. The STAT model does not predict fuel temperatures. A feature of the code is its brief input.

The STAT code uses two correlations to provide two independent estimates of the CHF at each axial location of each fuel rod surface. The McAdams correlation, which is provided by equation (14-6) on page 392 of Reference 4, is: $(q/A)_p = 400{,}000\ V^{1/3} + 4800\ (t_{sat} - t)\ V^{1/3}$, where $(q/A)_p$ is the critical heat flux in Btu/hr-ft^2, V is the liquid velocity in ft/s, t_{sat} is the saturation temperature of the water, and t is the local bulk coolant temperature of the water. Both temperatures are in Fahrenheit. Reference 4 indicates that the source of this correlation is Reference 5. The correlation is based on experiments in which water flows in an annulus formed by a heated rod of 0.25 inches in diameter centered inside a glass tube, which is 0.77 inches in inner diameter. The later reference provides the McAdams correlation as equation (15) and states: "The diameter of the annulus was not varied in the experiments on peak density of heat flux, hence the correlation applies only to the 0.25-inch heater in the 0.77-inch glass tube." Although this does not describe the situation in a TRIGA reactor core, it may be useful to compare the values of CHF obtained with this correlation with those obtained with the other CHF correlation in STAT, the Bernath correlation. Bernath[6] considered the data of many experimenters, including McAdams[5], to develop and test his correlation. STAT results tend to show that for TRIGA reactors the Bernath correlation, which is described in greater detail below, predict lower CHF values than does the McAdams correlation.

2.2 The RELAP5-3D Code[7] and Its Application to TRIGA Thermal-Hydraulic Analysis

Versions 2.3 and 2.4 of the RELAP5-3D code are available with certain restrictions on their use. An NRC version of the code, RELAP5/Mod3.2, is more generally available. Version 2.3 is available at Argonne National Laboratory (ANL) and was used in these analyses. The following discussion is focused on this version. The RELAP5-3D code is a general-purpose code capable of analyzing the transient coupled thermal, hydraulic, and neutronic behavior of light water nuclear reactors. It is a general-purpose code in the sense that it does not assume a prescribed geometry, but instead allows the user to connect a series of volumes of fluid nodes to each other to represent a channel or a series of connected channels and volumes.

Solid structures, called "heat structures" can be attached to the boundaries of the fluid volumes. These structures can be used to represent fuel elements, or tubes in a heat exchanger, or virtual any other heat absorbing, transferring, or generating structure. Each heat structure can consist of several layers of different materials. Thus, with the proper assembly of fluid volumes and heat structures, any of a large variety of systems can be simulated. As expected, the generality and flexibility of the code requires that a considerable amount of input is needed, even to represent a single coolant channel.

Because a major application of the RELAP5-3D code is the modeling of light water power reactors whose operating pressures are typically 1000 psia and above, its elaborate correlations for representing two-phase flow are more focused on this

application than on the very-low pressure (about 25 psia) application of pool-type research reactors. The pressure largely determines the increase in volume when liquid water boils and becomes steam. At 2000 psia the increase in volume is only a factor of 7.3, at 1000 psia it is a factor of 20.7, but at 25 psia it is a factor of 963. The large volume expansion at low pressures has substantial ramifications on the behavior of the flow.

RELAP5-3D comes with elaborate documentation in Acrobat (pdf) files that can be easily electronically searched. The code does not include the McAdams or the Bernath CHF correlations. However, the 1986 Groeneveld CHF look-up tables[8] and PG-CHF correlations[9,10] are available options. The former uses the 1986 AECL-UO Critical Heat Flux Lookup Table and the latter were developed by the Nuclear Research Institute Rez in the Czech Republic.

Figure 2 provides schematic view of the RELAP5-3D model used to represent a TRIGA coolant channel. The solid yellow (lighter-colored) regions that extend from the source at the top left to the sink on the top right represent the coolant, which flows for the source to the sink. Both the source and the sink are at the hydrostatic pressure at the depth at the top of the upper grid plate. The fuel rod and its upper and lower reflectors (darker-colored regions) are shown on the right side in contact with the coolant channel. The cold leg and the horizontal connector are at the reactor inlet temperature, which is also the temperature of the pool beyond of the reactor region. In the RELAP5-3D input the frictional resistance has been set to zero along the cold leg and the horizontal connector. These assumptions have the effect of applying the local hydrostatic pressure of the pool at the elevation of the lower reflector inlet to the lower reflector inlet. The source could have been attached directly to the lower reflector inlet and the cold leg and the horizontal connector could have been eliminated, but then a sufficiently accuracy value of the source pressure would have had to have been determined via an independent calculation. The horizontal connector in the model does not affect the flow rate and was included only for aesthetics. The fuel pin and the coolant channel in the fuel region were each divided into 15 equal horizontal layers, or nodes, and the upper reflector was divided into two equal layers, as shown in the figure.

The RELAP5-3D model nodal structure for the channel was selected to essentially agree with those of sample STAT model inputs provided by General Atomics. The coolant nodes of the lower reflector, fuel pin, upper reflector, and chimney are assumed to have the same flow area, wetted perimeter, and hydraulic diameter. The chimney length is merely the channel length where the fuel rods pass through the upper grid plate, or top handle in the case of conversion reactors. The lengths of each of these four regions were selected to mimic those used in the STAT modeling. In the RELAP5-3D model the hydraulic form losses (i.e., K-losses) were applied at the inlet to the lower reflector and at the outlet of the chimney node to mimic those used in STAT. Thus, the geometry and the hydraulic parameters of each RELAP5-3D model were chosen to mimic their STAT model counterparts. The STAT model does not use the cold leg or the horizontal connector node. It uses the equivalent approach of applying the appropriate pressures at the channel inlet and outlet.

2.3 Comparison of STAT and RELAP5-3D Flow Results

GA provided sample input and output files for the STAT code to facilitate the use of the code. The FORTRAN source code was also provided. Sample files for a hexagonal pitch TRIGA reactor operating at 2.0 MW and a rectangular pitch TRIGA reactor operating at 1.0 MW were included. Since 2.0 MW is at or near the highest power for which TRIGA reactors that rely on natural convection for their primary flow are allowed to operate, this reactor was chosen for use in the comparison of the STAT and RELAP5-3D codes. Table 1 provides key thermal-hydraulic parameters for these two reactors. Since it will be used in future calculations, the axial power distribution for the hexagonal pitch TRIGA is provided in Figure 3. Some of these representative parameters do not descibe any particular reactor and should not be considered to be the most limiting for safety analysis. For example, for convenience the hexagonal pitch reactor is assumed to have 100 rods with the hottest rod generating 30 kW, exactly 50% more power than the average.

In the STAT and the RELAP5-3D modeling, the shape of the coolant channel is not directly included. It does not matter that the fuel rods are on a triangular (or hexagonal) pitch in one reactor and on a rectangular pitch in the other. In this regard, in the STAT and RELAP5-3D models only the hydraulic diameter* and the flow area matter.

An important input parameter in the STAT code is the "void detachment fraction" (VDF). This quantity affects the buoyancy term in the hydraulic solution that is used to determine the flow rate. It has values between 0 and 1. A value of 0 implies that all of the steam or water vapor voids in the coolant remain attached to the fuel rod surfaces and do not contribute to the buoyancy of the flow stream. A value of 1 implies that all of the voids detach and contribute to the buoyancy of the flow stream. A brief study of the effect of the value of VDF was performed with the STAT code for the rectangular pitch TRIGA of Table 1. Table 2, which indicates the reactor power at which the Bernath correlation predicts that CHF would first occur, shows that the CHF power for a VDF of 1 is 27% greater than that for a VDF of 0.

Figure 4 provides a comparison of STAT and RELAP5-3D flow rate predictions. The vertical dashed line at 30 kW per rod corresponds to full power for the reactor. For the STAT calculation the most conservative void detachment factor value, 0, was used. The specific calculated data points are shown on the graphs. The interior color of three symbols for the STAT code is shown in white to identify a warning provided with the solution. The code indicates that the results are suspect when the outlet coolant temperature is within 11° F of the coolant saturation temperature.

The maximum power for the RELAP5-3D prediction, 48 kW per rod, is the highest power for which a solution was obtained. RELAP5-3D finds steady-state

* The hydraulic diameter, which is sometimes called the "equivalent diameter", is by definition four times the channel's flow area divided by the channel's wetted perimeter. This is used in determining hydraulic resistance. For a tube of circular cross section, the hydraulic diameter is the tube diameter.

solutions by solving a pseudo-transient in which there are no changes in the boundary conditions and forcing functions. An initial guess is the starting point. A steady-state solution is obtained when there are essentially no further changes in any dependent variable with time. The 48 kW/rod pseudo-transient solution has permanent minor oscillations in flow, which were on the order of 1% from minimum to maximum. When solutions were attempted at higher power levels, the amplitudes of the oscillations increased and sometimes caused the solution to end prematurely. The cause of these oscillations, which could be physical or an artifact of the calculation, requires further investigation. Vapor was first observed at a power of 30 kW per rod and produced a maximum void fraction of 1.22%. The maximum void fraction increased steadily with power until at 48 kW per rod it was 7.70%. In every solution attempt where flow oscillations were present, void fraction oscillations were also present. The two forms of oscillation are probably related.

During the discussion of the Figure 2 RELAP5-3D model in Section 2.2, it was suggested that an alternative model can be obtained by eliminating the cold leg and the horizontal connector and connecting the source node, with an appropriately adjusted pressure, directly to the lower reflector inlet. It was suggested that this alternative model would be less prone to the above flow oscillations. A Figure 2-style model of a square pitch TRIGA reactor had already been used to investigate flow oscillations. This model produced a stable steady-state solution at a power of 50.935 kW per rod and an oscillatory one at 52.0 kW per rod. First, the alternative model was used to essentially replicate the stable results at 50.935 kW per rod. The new model produced a steady-state flow that was only about 0.02% greater than that produced by the original model. Next, the power in the rod was increased to 52.0 kW in the alternative model. This caused a permanent flow oscillation, which varied about 3% between the minimum flow and the maximum. Thus, the alternative model appears to be as prone to flow oscillations as the original Figure 2 model.

The STAT flow results indicate that about 33 kW/rod the flow rate reaches a maximum and decreases thereafter. This is to be contrasted with the RELAP5-3D results which indicate that the flow rate increases monotonically to at least 48 kW per rod. The downturn in flow predicted by the STAT code is suspect because, as explained above, it occurs where the code predicts an outlet temperature that is within 11°F of the saturation temperature. While the STAT and RELAP5-3D results are essentially equal at 10 kW per rod, the RELAP5-3D flow rate is significantly greater than the STAT flow at 30 kW per rod.

Figure 5 provides the STAT versus RELAP5-3D channel outlet coolant temperatures that correspond to the Figure 4 flow rates. Since for a fixed power, the coolant temperature rise is essentially inversely proportional to the flow rate until the coolant saturation temperature is reach, the results are as expected with the STAT outlet temperatures greater than the RELAP5-3D temperatures. The last two points on the STAT curve are at the saturation temperature of 114.8° C. STAT predicts CHF to first occur at 37.1 kW per rod, which corresponds to the last point on the STAT plot.

3 CRITICAL HEAT FLUX

Published values of CHF for various flow channels are based almost exclusively on measurements made in facilities designed specifically for CHF measurement. Many investigators have made measurements of critical heat flux in water and in other fluids. Many geometries, including tubes, annuli, and rod bundles have been tested. CHF is a very difficult quantity to measure accurately. Independent measurements of CHF for the same geometry and set of fluid conditions can vary significantly. There can be considerable scatter in a set of measurements by a single investigator.

Most critical heat flux measurements are made with a uniform heat flux over the length of the channel. Because nuclear reactors have heat fluxes that vary along the lengths of the coolant channels, some means is needed to adapt the CHF data that was measured with a uniform heat flux to the reactor situation. Both the STAT and the RELAP5-3D codes accomplish this by use the direct substitution method. If a given set of pressure, mass flow rate (flow per unit area), and quality/temperature values produced a particular value of CHF in the experiment, it is assumed that this set will produce the same value of CHF if the same set of conditions occurs at any given location in the reactor. The ratio of the predicted CHF to the local value of heat flux in the reactor is defined to be the CHF ratio at that location. The power that causes the minimum CHF ratio among all locations to be 1.0 is the CHF power.

Table 3 shows the approximate ranges of key parameters needed to predict CHF in TRIGA reactors. There is a lack of measured CHF data in these ranges of the parameters. Much of the work in CHF data measurement has been directed at power reactors. The mass flow rates and operating pressures of power reactors typically are much higher than those of TRIGA reactors.

The specific CHF correlations, including formulas, look-up tables, and other methodologies for determining CHF that are considered in this report are:

1. Bernath (1960)[6] –Used in the STAT code along with McAdams (1949).[5]
2. 1986 Version of the Groeneveld Tables[8] – A RELAP5-3D Version 2.3 option.
3. 1995 and 2006 Version of the Groeneveld Tables[11,12,13] – Updated versions of the 1986 Groeneveld tables that are not available in RELAP5-3D Version 2.3.
4. Hall and Mudawar (Purdue)[14,15,16] – A proprietary circa 1998 collection of the world's CHF data in water. For non-uniform heat flux, they provide a simple correlation for subcooled boiling.
5. PG-CHF (Czech Republic, circa 1994)[9,10] – A RELAP5-3D Version 2.3 option that has four correlation options for rod bundles.

3.1 Bernath CHF Correlation

The Bernath correlation, as used in the STAT code, is describe in Reference 6 and is given by:

$$(Q/A)_{BO} = h_{BO}\left(T_{w_{BO}} - T_b\right)$$

$$h_{BO} = 10890\left(\frac{D_e}{D_e + D_i}\right) + (\text{slope})\ V$$

$$\text{slope} = 48/D_e^{0.6} \quad \text{if } D_e \le 0.1 \text{ ft}$$

$$\text{slope} = 90 + 10/D_e \quad \text{if } D_e > 0.1 \text{ ft}$$

$$T_{w_{BO}} = 57 \ln P - 54\left(\frac{P}{P+15}\right) - \frac{V}{4}$$

where $(Q/A)_{BO}$ is the CHF heat flux in p.c.u.[†]/hr-ft^2 (BO stands for "burnout"), h_{BO} is the heat transfer coefficient corresponding to the CHF in p.c.u./hr-ft^2-C, $T_{w_{BO}}$ is the wall temperature at which CHF occurs in °C, T_b is the local bulk coolant temperature in °C, D_e hydraulic diameter of the coolant passage in feet, D_i is the diameter of the heater surface (heated perimeter divided by π) in feet, P is the pressure in psia, and V is the velocity of the coolant in ft/s.

Bernath based the above correlation on the measured data of McAdams[5] and the measured data of Columbia University.[17] Both sets of experiments were at low pressure and measured CHF for subcooled boiling in annuli. McAdams used a 0.25-inch heater inside a 0.77-inch tube, which corresponds to a hydraulic diameter of 13.2 mm. Columbia used a 1.08-inch diameter heater inside various unheated tubes. There were 14 Columbia tests. The approximate ranges of the Columbia test variables were: pressure – 2 to 4 bars, local bulk coolant temperature – 80 to 110° C, mass flow rate – 1800 to 9000 kg/m^2-s (6 to 30 ft/s), hydraulic diameter – 10.6 to 14.7 mm. Bernath also compared his correlation with several other sets of independently measured data covering a wide range of parameters. None of these additional sets of data closely match TRIGA conditions. In particular, with the exception of the McAdams test, the lowest mass flow rates in the tests are about an order of magnitude too high. The velocities in the McAdams tests are 1, 4, and 12 ft/s. However, Bernath discredits all of the McAdams 1 ft/s tests as not being representative of the group of McAdams tests and as having experienced premature burnout.

The Bernath correlation can predict unreasonable values of CHF for low pressure bulk boiling. Bulk boiling implies that the mixed-mean coolant temperature is at the saturation temperature and liquid and vapor are present in the coolant stream. The presence of steam, which has a very low density at low pressure, implies that the average density of the water and vapor taken together is much lower than when only liquid is present in the stream. The much lower average density causes a much higher average

[†]A p.c.u. is a "pound centigrade unit" and is defined to be the amount of energy required to raise one pound of water one degree Celsius. This is to be compared to a Btu, which is the amount of energy required to raise one pound of water one degree Fahrenheit. Thus, 1 p.c.u. is equal to 1.8 Btu's, since a degree Celsius equals 1.8 degrees Fahrenheit. It also follows that a p.c.u. per degree C equals a Btu per degree F. The McAdams and Bernath correlations as programmed into the STAT code provide CHF in units of Btu/hr-ft^2.

velocity. This causes the V/4 term in the above equation for $T_{W_{BO}}$ to be relatively large and can make the local wall temperature less than the local bulk coolant temperature. This makes no sense and produces negative values of CHF.

3.2 Groeneveld Tables

Goeneveld et al. attempted to collects the world's data for CHF in water and produced a CHF look-up table that he published in 1986.[8] For example, a table is provided that corresponds to a pressure of 100 kPa (1 bar) in which successive rows represent increasing values of mass flux (kg/m^2-s) and successive columns represent increasing values of water quality in increments between -0.15 and 0.90.[‡] For each combination of mass flow rate and quality there is a value of CHF (kW/m^2). Many similar tables are provided to cover a pressure range of 100 kPa to 20000 kPa. For conditions between table entries and between tables of constant pressure linear interpolation is used.

The entire Groeneveld table data corresponds to a uniformly heated round tube of internal diameter of 8-mm. The heat is assumed to be provided to the inner surface of the tube and to be removed by water flowing inside the tube. For all other geometries and conditions, Groeneveld provides factors. Six are defined in Reference 8. Hence for a TRIGA rod bundle the CHF, CHF_{BUNDLE} is given by:

$$CHF_{BUNDLE} = CHF_{TABLE} \times K_1 \times K_2 \times K_3 \times K_4 \times K_5 \times K_6$$

where CHF_{TABLE} is the value interpolated from the Groeneveld tables, which corresponds to a 8-mm diameter tube, and K_1 through K_6 are multiplicative factors to account for such things as the diameter being other than 8 mm, rod bundle versus tube geometry, the presence of grid spacers, and stratified horizontal flow. K_1 is the factor to use when the hydraulic diameter is not 8 mm. It is given as:

$$K_1 = \left(\frac{8}{D}\right)^{1/3} \quad \text{for } 2 < D < 16$$

$$K_1 = \left(\frac{8}{16}\right)^{1/3} = 0.79 \quad \text{for } D > 16$$

where D is the hydraulic diameter of the channel in mm. K_2 is the factor to account for rod-bundle geometry rather than tube geometry. It is a function of quality, X, and is given by:

$$K_2 = \min\left[0.8,\ 0.8\exp\left(-0.5\,X^{1/3}\right)\right]$$

Thus, for negative values of X, which corresponds to subcooled conditions, K_2 is 0.8. When X is positive, K_2 is smaller than 0.8. Most of the other factors should be close to 1.0 and are 1.0 when they are not applicable, such as the grid spacer factor K_3, when

[‡] A brief description of coolant quality is provided in Appendix A.

there are no grid spacers. K_4 is the heated length factor, which enhances the value of CHF near the channel entrance. K_5 is the axial flux distribution factor, which is 1 when the quality, X, is less than zero and is the heat flux averaged over the boiling length (the length from X=0 to $X=X_{CHF}$) divided by the local heat flux for qualities greater than 0. K_6 is a flow factor which for vertical flow can be used to correct CHF for downward flows and some upward flow conditions for which the mass flow is less than 100 kg/m^2-s.

Based on the source code and the input manual for RELAP5-3D Version 2.3, K_4 is obtained from the following algorithm:

$$\text{if } X < 0, X = 0$$

$$\text{if } \frac{L}{D} < 5, \frac{L}{D} = 5$$

$$\alpha = \frac{X}{X + \rho_g (1 - X)/\rho_f}$$

$$K_4 = \exp\left(\frac{D}{L}\exp(2\,\alpha)\right)$$

where X is the quality, L is the heated distance from the inlet of the channel, and D is the heated diameter (4 × the flow area / the heated perimeter). For qualities less than or equal to 0, this formulation causes α to be 0 and K_4 to be no greater than 1.22. However, for slightly positive qualities, K_4 can be larger than 2. For example, Figure 6 shows K_4 for the middle axial node of the hexagonal pitch TRIGA reactor as a function of quality.

In 1995 Groeneveld revised the table values and discussed other options for K_1. The table was revised again in 2003[12] and in 2005.[18] In 2005 Reference 12 revised the K-factors and identified some as tentative. K_4 was not changed. An additional K-factor, which is a radial or circumferential flux distribution K-factor, was added. Reference 12 recommends the following relationship for K_1:

$$K_1 = \left(\frac{8}{D}\right)^{1/2} \quad \text{for } 3 < D < 25$$

$$K_1 = \left(\frac{8}{25}\right)^{1/2} = 0.57 \quad \text{for } D > 25$$

For the 18.64 mm hydraulic diameter of the hexagonal pitch TRIGA reactor the 1986 relationship for K_1 produces a value of 0.79 while the 2005 one produces a value of only 0.66. This change causes the new K_1 to be 83% of the 1986 value.

The complete 1986 Groeneveld table is included in Reference 8. The complete 1995 Groeneveld table was at one time available over the internet. Values for the 2006 Groeneveld table can be found in Reference 13. For the current study K_1, K_2, and K_4 will be assumed to be as defined above with the 1986 relationship for K_1 used with the 1986

Groeneveld table and the later, Reference 12, K_1 used with the 1995 and 2006 versions. All other K values will be assumed to be 1.0.

3.3 Hall and Mudawar (Purdue) Correlation

Hall and Mudawar, who are at Purdue University, have compiled and assessed the world's CHF data for water and have produce simple correlations for subcooled water flowing inside a tube that is heated from the outside.[14,15,16] Initially, the authors intended is to make the database that they generated publicly available. However, an email response from Mudawar indicates that they chose to keep it proprietary. For applications where the axial distribution of heat flux is not uniform, they recommend their "outlet" CHF correlation, which is the following:

$$Bo = C_1 We_D^{C_2} \left(\frac{\rho_f}{\rho_g}\right)^{C_3} \left[1 - C_4 \left(\frac{\rho_f}{\rho_g}\right)^{C_5} x_0\right]$$

where:

Bo is the boiling number, which is given by CHF/(G h_{fg}).

We_D is the Weber number, which is given by G^2 D /(ρ_f σ)

ρ_f and ρ_g are the density of the saturated liquid and vapor, respectively.
x_o is the thermodynamic equilibrium quality, (h − h_f)/h_{fg}, with saturated thermophysical properties evaluated at the pressure associate with the CHF data point (usually outlet pressure). The subscript "o" refers to the outlet of the heated length. h is enthalpy. h_f is the enthalpy of saturated liquid.

$C_1 = 0.0722$; $C_2 = -0.312$; $C_3 = -0.644$; $C_4 = 0.900$; $C_5 = 0.724$

G is the mass flow rate

h_{fg} is the heat of vaporization.

D is the inside diameter of the tube, which is also the hydraulic, or equivalent, diameter.

σ is the surface tension.

The authors obtained the above correlation as a fit to a portion of the data in their data base. They indicate that the range of applicability of the data is D between 0.25 and 15 mm, G between 300 and 30,000 kg/m^2-s, pressure between 1 and 200 bar, and quality (x_0) between −1.00 and −0.05. Thus, the TRIGA hydraulic diameters above 15 mm are out of range. The mass flow rate of TRIGA reactors at normal operating condition of about 180 kg/m^2-s is below the range of the correlation. The TRIGA mass flow rate at

CHF conditions may also be below the 300 kg/m^2-s bottom of the range. Qualities above −0.05 are out of range.

3.4 Comparison of Bernath, Groeneveld, and Purdue CHF Correlations for Fluid Conditions Representative of TRIGA Reactors

The Groeneveld tables are for an 8 mm tube that is uniformly heated from the exterior and cooled on the interior. The lowest value of mass flow for which the Purdue correlation is applicable is 300 kg/m^2-s. The rectangular pitch TRIGA reactor operates at 1.8 bar. Therefore, Figure 7 provides critical heat flux as a function of water temperature for these conditions based on the Bernath, Groeneveld, and Purdue correlations. The three Groeneveld correlation curves are similar in shape. The 2006 curve, which is the smoothest of the three, produces lower values over the range of the plot than does the other three. The Purdue curve ends at 90.8° C, which corresponds to a quality of −0.05, which is the limit of the correlation. The other four curves end at 116.9° C, which is the saturation temperature.

Figure 8 is similar to Figure 7. It provides quality instead of temperature along the abscissa. This allows positive values for quality to be represented. The fundamental relationship between quality and enthalpy and between quality and temperature are briefly described in Appendix A. The coolant temperature corresponding to each value of quality is shown along the abscissa of Figure 8.

Figure 9 is the same as Figure 7, except that it provides CHF values for a 19.65 mm diameter tube instead of an 8 mm one. The 19.65 mm diameter tube was chosen to correspond to the hydraulic diameter of the rectangular pitch TRIGA reactor. The larger diameter causes the 1995 and 2006 Groeneveld table CHF values at each value of temperature to be considerably below the 1986 value. This is due to the change in K_1, the diameter factor, after 1986.

3.5 Comparison of Bernath, Groeneveld, and Purdue CHF Predictions for the Hexagonal Pitch TRIGA Reactor

The hottest rod in the hexagonal pitch TRIGA reactor, operating at nominal conditions, has a power of 30 kW. The CHF ratios on the surface of this rod operating at this power were evaluated with the STAT and the RELAP5-3D codes. The red curve with the "x" symbols in Figure 10 shows the axial distribution of CHF ratio as obtained directly from the STAT code. The rightmost green curve with the triangle symbols shows the 1986 Groeneveld results from RELAP5-3D. The other two CHF curves, which are in between these two curves, show the RELAP5-3D thermal hydraulic solution coupled with either the Bernath correlation or the 2006 Groeneveld table. Because RELAP5-3D does not include either of these correlations, these two CHF curves were obtained via hand calculations, which were performed with the aid of a computer spreadsheet. The 1986 Groeneveld values of CHF were also calculated with a spreadsheet as a check on the methodology used to obtain the 2006 results. The hand calculated 1986 CHF values were within about 0.5% of the values calculated by

RELAP5-3D. The numbers next to the diamond symbol of the green curve at the far left show the axial distribution of K_4. These values were used in the determination of all of the Groeneveld CHF values in the figure.

Figure 10 can be used to predict the CHF power of the hottest rod for each correlation by multiplying the minimum CHF ratio from each curve by 30 kW. However, there is a major shortcoming in this approach. It is only valid when the minimum CHF ratio is 1.0. This point is demonstrated with Figure 11. The thick red curve with the triangle symbols shows flow versus power, as predicted by RELAP5-3D for the hexagonal pitch TRIGA. The same red curve is shown in Figure 4 with power along the abscissa and flow along the ordinate.

The top curve in Figure 11, which is labeled "CHF Power Based on RELAP5-3D Conditions", shows the CHF power that RELAP5-3D would have been predicted if the 2006 Groeneveld table were included in RELAP5-3D. This curve, which is based on the RELAP5-3D power and flow rate curve, shows that the predicted value of CHF power changes as the RELAP5-3D power and flow change. In the reactor there can be only one power at which CHF first occurs. This power must be the power at which the CHF power and the RELAP5-3D power used to predict it are the same. Hence, it must be at the intersection of the thin blue upper curve and the red curve. Unfortunately, as explained above, RELAP5-3D starts to produce oscillatory flows at 48 kW per rod. Therefore, the last five points of the red RELAP5-3D flow curve were used in a least-square linear fit to extrapolate the curve, as indicated by the dashed red line. In a similar manner the upper curve with the "x" symbols was also extrapolated.

Perhaps, the best approach to predicting CHF power is represented by the thick blue curve with the yellow diamond symbols in Figure 11. For each value of flow, the power at which CHF first occurs can be calculated without the use of RELAP5-3D or any other code of similar sophistication. The inlet temperature, axial power shape, and coolant pressure are known. An energy balance can be used to calculate coolant enthalpy and quality along the length of channel for any assumed value of channel power. This enables values of CHF and CHF ratio (i.e., CHF divided by local heat flux) to be calculated along the length of the channel for the assumed channel power. The assumed channel power can be adjusted until the minimum CHF ratio along the length of the channel is 1.00. This power is the CHF power for that flow. The thick blue line, labeled "Minimum CHF Ratio = 1.0", shows the CHF power as a function of flow.

If the flow rate at which CHF occurs were known, the CHF power could be read directly from "Minimum CHF Ratio = 1.0" curve of Figure 11 at that flow. Therefore, the predicted 2006 Groeneveld CHF power based on the extrapolated RELAP5-3D flow is at the intersection the thick blue curve and the extrapolated RELAP5-3D flow curve, where the hottest rod has a power of 68.9 kW. A more appropriate choice is along the thick blue curve at the flow rate where the RELAP5-3D code results end, 0.1394 kg/s, since the behavior beyond this flow could be due to physical phenomena or to a RELAP5-3D code issue. This flow yields a CHF power of 62.1 kW per rod. (All three curves in Figure 11 would have intersected at the same point if the extrapolated portion

of the upper blue curve with the "x" symbols were calculated based on the extrapolated RELAP5-3D flow curve.)

A feature of the latter approach is that the relationship between equilibrium CHF power and flow (the thick blue curve) is independent of the relationship between channel (or reactor) power and flow (the thick red curve). This makes it easy to replace either relationship with another one. For example, the RELAP5-3D relationship between power and flow can be replaced with the STAT relationship or with a new RELAP5-3D relationship based on revised inlet and outlet form-losses, or K-losses. Also, the thick blue CHF curve based on the 2006 Groeneveld tables can be replaced with one based on another CHF relationship.

Intuitively with regard to the calculations of the "Minimum CHF Ratio = 1.0" curve of Figure 11, one would expect that for a specific channel flow rate the minimum CHF ratio would decrease monotonically as the assumed channel power is increased. This is generally true except for the effect of K_4, Figure 6, as the quality goes from negative to a small positive value. This is where the rapid increase in K_4 with only a modest increase in quality, which is caused by only a modest increase in power, causes a substantial increase in CHF and CHF ratio. In these regions there can be temporary increases in minimum CHF ratio with increasing channel power before the decline resumes. Thus, there can be a local minimum followed by a local maximum. If the local minimum is less than 1.0 and the local maximum is greater than 1.0, then there will be three values of channel power where the minimum CHF ratio is 1.0. The second and third points (from the left) of Figure 11 showed this behavior. For the second point (0.0799 kg/s) the local minimum CHF ratio, 0.9824, occurred at 47.487 kW/rod and the local maximum, 1.1083, occurred at 47.770 kW/rod. The three solutions, where the minimum CHF ratio is 1.0, are 47.300, 47.537, and 50.522 kW/rod. The third point (0.1001 kg/s) displayed similar behavior and produced solutions 52.383, 52.899, and 53.339 kW/rod. In each case the lowest power of the three values is obviously the one where a minimum CHF ratio of 1.0 is predicted to occur first. In an earlier version of Figure 11, Figure 8 of Reference 19, the two lower valued solutions for each of these flow rates were missed and only the highest value was plotted.

Figure 12 is analogous to Figure 11, except that the Bernath correlation was used in place of the 2006 Groeneveld correlation. In addition the STAT prediction of channel power versus flow rate, as provided in Figure 4, has been included. The intersection of the "Minimum CHF Ratio = 1.0" and extrapolated RELAP5-3D curves produces a predicted CHF power of 51.7 kW/rod. This is about 2% greater than the value of 50.6 kW/rod indicated in Table 2 of Reference 19. This difference is due to a small error in the calculation that was subsequently corrected.

Figure 13 shows the CHF power versus flow predictions for the hexagonal pitch TRIGA reactor based on the "outlet" CHF correlation by Hall and Mudawar from Purdue. The RELAP5-3D flow versus power relationship is also repeated. The predicted CHF power, 50.6 kW per rod, is at the intersection of the CHF and extrapolated RELAP5-3D curves, where the flow is 0.145 kg/s. The corresponding mass flow is 265 kg/s-m^2. At

the limiting axial location along the fuel rod, where the CHF ratio is 1, the coolant quality is −0.02. Since the mass flux is less than 300 kg/s-m^2, the quality is greater than −0.05, and the hydraulic diameter is greater than 15 mm, the conditions used to predict the CHF power are clearly beyond the range of the Hall and Mudawar "outlet" CHF correlation.

3.6 PG-CHF CHF Correlations

The PG-CHF CHF correlations and the 1986 Groeneveld table are the only CHF options built into the RELAP5-3D Version 2.3 and 2.4 codes. The PG-CHF correlations are based on three separate experimental databases – one for tubes, one for rod bundles, and one for annuli. For each of these three geometries there are four forms of the PG_CHF correlation – "Basic", "Flux", "Geometry", and "Power". The rod bundle database is based on 153 test geometries and 7,616 data points.[9]

The range of applicability for some of the key parameters for the rod bundle correlations are: pressure between 2.8 and 187.3 bar, mass flux between 34.1 and 7478 kg/m^2-s, quality between subcooled and 100% steam, heated length between 0.4 and 7.0 m, and fuel rod diameter between 5 and 19.05 mm. Thus, the TRIGA pressure of about 1.8 bar is too low, the heated length of 0.381 m is too short, and the rod diameter of about 37 mm is much too large. However, since the PG-CHF rod bundle CHF correlations are a RELAP5-3D option that apparently are based on measurements in rod bundles, they were included in the current study.

When the "Basic", "Flux", "Geometry" versions of the rod bundle PG-CHF were selected, RELAP5-3D Version 2.3 produced obviously erroneous values of the rod heat flux distribution. Therefore, the PG-CHF results were manually calculated with the aid of a spreadsheet. The algorithms for these correlations, which are quite complex, were obtained from Reference 9 with the aid of Volume IV of the RELAP5-3D Version 2.3 manual. The manually calculated results for the "Power" option agreed with the RELAP5-3D results.

Figure 14, which is analogous to Figure 10, shows the PG-CHF CHF results for the hexagonal pitch TRIGA evaluated at a rod power of 30 kW. The Bernath (STAT) curve and the 1986 Groeneveld (RELAP5-3D) curves of Figure 10 are included for purposes of comparison. The "Geometry" PG-CHF curve, which is pink with white diamond symbols, is essentially coincident with the "Flux" curve. The large difference between the "Power" CHF prediction and the other three PG-CHF predictions in Figure 14 do not appear in Figure 15, which is analogous to Figure 13. Thus, these CHF differences essentially disappear when the CHF power is evaluated at the channel power, i.e., at the power which makes the minimum CHF ratio 1.0. The PG-CHF correlations were designed so that when the channel power equals the CHF power, the "Power" and "Flux" correlations yield the same results. For purposes of verification, the curves of both of these were calculated individually for Figure 15. They produced identical results. Portions of the "Geometry" curve are barely visible above the "Power and Flux" curve.

4 DISCUSSION

4.1 Comparison of CHF Predictions for the Hexagonal Pitch TRIGA Reactor

Figure 16 combines many of the curves of Figures 11, 12, 13, and 15 in a single figure. The basic and geometry versions of the PG-CHF CHF curves were excluded because they are very close to the power and flux versions. There are many options for predicting CHF power in the hexagonal pitch TRIGA. In the past General Atomics has used the STAT code, which they developed, along with the Bernath correlation, which is incorporated into the code. The intersection of the STAT power-versus-flow relationship with the Bernath correlation occurs at the lower left of Figure 16 and produces a CHF power of about 37 kW/rod. The STAT code produced a value of 37.1 kW/rod for a CHF ratio of 1.0.

Table 4 summarizes values of CHF per rod for nine combinations of CHF correlation and thermal-hydraulics code. In the table, combination options A, B, and C are shown in separate columns, where A, B and C are:

- A: CHF curve at maximum calculated RELAP5-3D rod flow of 0.1394 kg/s (thin vertical black line in Figure 16.)
- B: Intersection of CHF curve with STAT or extrapolated RELAP5-3D flow curve
- C: CHF predictions based on 30 kW per rod and the corresponding STAT or RELAP5-3D calculated flow. (These are based on the minimum CHF ratios of Figures 10 and 14.)

Since the power of the hottest rod for nominal full power operation in the hexagonal pitch TRIGA reactor is 30 kW, the CHF ratios shown in the table are the CHF powers divided by 30 kW.

Option C is an inappropriate choice because it uses a power of 30 kW/rod to predict a CHF power that can be much higher. When the assumed 30 kW per rod is increased, the predicted CHF power often decreases. Only the equilibrium (minimum CHF ratio = 1.0) condition, where the two powers are equal, is appropriate. The choice of option A over the less conservative option B is a judgment call. Option A is probably the better choice, especially when the difference in predicted CHF power is small and the difference between the flow at the intersection point and the maximum calculated flow is large.

Figure 16 and Table 4 show a wide variation among the curves of predicted CHF power. A cause of this is that the measured data underpinning the Bernath, Purdue, and PG-CHF correlations do not closing match the conditions applicable to TRIGA reactors.

The thick black straight dashed line in Figure 16, labeled "Exit Quality = 0", shows the combinations of power and flow that produce a mixed-mean quality of 0 at the exit of the limiting hexagonal pitch TRIGA channel. The PG-CHF correlations predict that CHF occurs with bulk boiling at the channel exit. The Purdue and Bernath correlations intersect the extrapolated RELAP5-3D flow curve below the "Exit Quality = 0" line. The Groeneveld 2006 CHF intersection with the RELAP5-3D flow curve is essentially on the "Exit Quality = 0" line, as is the STAT-Bernath intersection. Mass flux, G, which is linear with flow rate, is used in some of the correlations. Figure 16 indicates that the values of G at flows of 0.1 and 0.3 kg/s are 183 and 549 kg/s-m^2, respectively.

4.2 STAT versus RELAP5-3D

Figure 16 enables the RELAP5-3D and STAT flow predictions to be compared along with their effects on the predicted value of CHF power. In this comparison STAT is the more conservative choice. For this comparison, the most conservative void detachment fraction of 0 was used in the STAT code. Void detachment fraction is not an applicable concept for the RELAP5-3D code.

The RELAP5-3D analytical model is more thoroughly documented than is the STAT model. Various versions of the RELAP5-3D code are more readily available than is the STAT code. Accordingly, RELAP5-3D is, in general, more widely used and understood by analysts outside of General Atomics.

RELAP5-3D is a general purpose steady-state and transient code that can predict fuel temperature, as well as coolant conditions. STAT is a steady-state code that cannot predict fuel temperatures. The limited focus of STAT enables its input to be relatively simple. The input for the RELAP5-3D model of a TRIGA reactor is quite complex. A mitigating factor is that the RELAP5-3D model for one TRIGA reactor can be adapted to represent another TRIGA reactor with much less effort than was required to produced the original RELAP5-3D model.

The STAT code has been used in the safety analyses of nearly all TRIGA reactors. The RELAP5-3D code has had limited use in this regard.

The comparison of RELAP5-3D and STAT flow predictions validates neither code for analysis of TRIGA reactors. Validation must come from measured data. Entrance and exit K-losses are an issue which is addressed in Reference 1. Changes in these parameters will affect the STAT and RELAP5-3D power versus flow curves and thereby influence the predicted values of CHF power obtained from each CHF power versus flow curve for the hexagonal pitch TRIGA reactor.

4.3 Choosing an Acceptable Minimum Margin to CHF

The 2006 Groeneveld correlation is judged to be the best choice of all of the correlations known to be available. However, it is not recommended to use the 2006 Groeneveld CHF correlation alone for calculating CHF in TRIGA reactors because the

amount of measured data is insufficient to determine a definitive conclusion as to the power level at which CHF occurs.

The 2006 Groeneveld correlation is the newest and incorporates the world's CHF data in water. In regions of the 2006 Groeneveld table where measured data is lacking it makes use of CHF values predicted by CHF correlations, such as those provide by Hall and Mudawar (Purdue University), Reference 15. Thus, some of the Purdue data is, in effect, included in the 2006 Groeneveld table.

The cells in the 2006 Groeneveld table use four levels of shading to highlight regions of uncertainty. The values in unshaded cells were obtained from measurement and therefore have the least uncertainty. The lightly shade cells represent extrapolation. The other two darker regions include conditions where CHF is difficult to measure or rapid changes in CHF occur with moderate changes in quality. The regions of the table needed for predicting CHF in TRIGA reactors are lightly shaded. The uncertainty for these regions depends on the amount of extrapolation from data-based regions.

Reference 13 uses smoothing methods to eliminate discontinuities that are a result of scatter in the measured data. The reference provides RMS errors between the measured data and the smoothed entries in the table. For the direct substitution method being used in the current analysis, negative qualities in the measured regions of the table have an RMS error of 14.74%. Positive quality regions have much higher RMS errors. Since the regions of the table applicable to TRIGA reactors are extrapolated from measured regions, the uncertainty could be significantly greater than that represented by an RMS error of 14.74%.

NUREG-1537, *Guidelines for Preparing and Reviewing Applications for the Licensing of Non-Power Reactors*, Part 1, Appendix 14.1, page 5 recommends CHF ratios of at least 2.0 for reactors with engineered cooling systems. TRIGA reactors with natural-convective cooling do not have engineered cooling systems. Past and current practice does not include hot channel factors or other uncertainty factors in the CHF analysis of TRIGA reactors that are cooled by natural convection. The possible exception here is the uncertainty in measured power.

The successful operation of more than 60 TRIGA reactors represents an important body of data. The utility of this data is largely dependent on the similarity of these reactors with regard to CHF performance. Reference 1 has used RELAP5/MOD3.2 to provide channel flow rate versus power data for the Washington State University (WSU), Texas A & M University (TAMU), the U. C. Davis McClellan Nuclear Radiation Center (MNRC), and Oregon State University (OSU) TRIGA reactors. TAMU and OSU have a peak rod power of about 17 kW at a reactor design power of 1.0 MW. WSU has a peak rod power of about 21 kW at a reactor design power that is also 1.0 MW. MNRC has operated at 2.0 MW. Reference 20 performed an analysis of the MNRC reactor operating at 2.0 MW with 101 fuel rods in which the peak rod power was 33.2 kW. WSU and TAMU have rectangular pitches, MNRC has a hexagonal grid plate, and OSU has a circular one. In the calculations each of the reactors was assumed to have an inlet

temperature of 30° C. This data is used in Appendix B to show that the power for each CHF correlation falls within a relatively narrow band with Bernath predicting between 40.4 and 56.5 kW per rod and 2006 Groeneveld predicting between 61.2 and 70.5 kW per rod.

4.4 Potential Flow Oscillations Prior to CHF

Although the flow oscillations observed in the RELAP5-3D calculations may not accurately represent the behavior of the channel flow, they may be indicative of a type of behavior that can occur in subcooled boiling, as described by the following scenario. Subcooled boiling generates vapor, which increases the buoyancy in the channel and, in turn, increases the channel flow rate. The increased flow rate, with a constant channel power, causes a reduction in channel coolant temperatures, which causes the voids to collapse as the vapor condenses back to liquid. When the voids collapse, the buoyancy decreases and causes the channel flow rate to decrease. This, in turn, causes the channel coolant temperatures to increase and the voids to reappear, thus completing the cycle. In the extreme, such oscillatory behavior is undesirable and could lead to significant oscillations in fuel rod temperature.

An oscillatory flow phenomenon, referred to as "chugging", has been observed experimentally. The CHF analysis for the Annular Core Research Reactor in Reference 21, which was performed by the Sandia National Laboratories in support of the upgrade of the reactor from 2.0-MW to 4.0-MW operation, employs measured CHF data from the University of New Mexico, Reference 22. This data was collected at a pressure of 1.18 bar and at mass flow rates between 0 and 260 kg/m^2-s. The University of New Mexico took CHF measurements in three annuli. Each annulus was formed by a 0.5-inch diameter heater, which had a 19.7-inch heated length and is concentrically located inside an unheated Pyrex tube. In the University of New Mexico tests chugging was observed to start at heat fluxes that were 40% of those that were observed to initiate CHF in the smallest annulus and were 88% in the largest.

The presence of oscillatory vapor-induced voids also has reactivity implications for TRIGA reactors. References 23 and 24 experimentally investigated a phenomenon that they also referred to as "chugging". This chugging is believed to be largely due to reactivity effects. Voids are generated, which adds negative reactivity. The negative reactivity causes a downward spike in power. The reduced power causes the voids to collapse, which, in turn, adds reactivity and increases the power back to normal. Then new voids are generated and the cycle repeats. To the extent that vapor-induced flow and power oscillations are a detectable precursor to CHF, they could serve as a warning that could enable CHF to be avoided.

5 CONCLUSIONS

Because of the lack of measured CHF data in the region of interest to TRIGA reactors, none of the CHF correlations considered can be assumed to provide the definitive power at which CHF will occur. In all cases considered, the 2006 Groeneveld

CHF table with factors K_1, K_2, and K_4, as described above, predicts substantially higher values of CHF power for TRIGA reactors than does the Bernath correlation. The Bernath correlation was developed in 1960 and has traditionally been used for predicting CHF in TRIGA reactors. The successful operation of more than 60 TRIGA reactors attests to their safe operation. Analytical data for four TRIGA reactors provided in Appendix B shows that when the 2006 Groeneveld CHF correlation is used without flow extrapolation (Method A), as prescribed above, the power per rod at which CHF is predicted to occur is expected to fall within a relatively narrow range, which is considerably higher than the range predicted when using the Bernath correlation.

In conclusion, it is recommended that in assessing the potential for CHF in a specific TRIGA reactor, the power of each of the potentially limiting rods in the reactor be compared with the power at which CHF is predicted to occur via 1) the Bernath correlation and 2) the 2006 Groeneveld correlation using Method A, as indicated above.

REFERENCES

1. J. Vic Del Bene, *TRIGA Reactor Thermal-Hydraulics Study, STAT-RELAP5 Comparison*, General Atomics report, to be issued.

2. "STAT – A Fortran Program for Calculating the Natural Convection Heat Transfer – Fluid Flow in an Array of Heated Cylinders," GEN-44, General Atomics, July, 1989.

3. J. F. Petersen, *Steady State Thermal Analysis for the Proposed Use of TRIGA Fuel Elements in MTR Reactors*, GA-5708, General Atomic, Division of General Dynamics, San Diego, California, April 15, 1965.

4. William H. McAdams, *Heat Transmission*, Third Edition, McGraw-Hill Book Company, Inc., New York, 1954.

5. W. H. McAdams, W. E. Kennel, C. S. Minden, Rudolf Carl, P. M. Picornell, and J. E. Dew, "Heat Transfer at High Rates to Water with Surface Boiling," *Industrial and Engineering Chemistry*, Vol. 41, No. 9, September 1949, pp. 1945-1953.

6. Louis Bernath, "A Theory of Local-Boiling Burnout and Its Application to Existing Data," *Chemical Engineering Progress Symposium*, Series No. 30, Volume 56, 1960, pp. 95-116.

7. The RELAP5-3D© Code Development Team, RELAP5-3D© Code Manual, Version 2.3, INEEL-EXT-98-00834, Idaho National Laboratory, April 2005.

8. D. C. Groeneveld, S. C. Cheng, and T. Doan, "1986 AECL-UO Critical Heat Flux Lookup Table," *Heat Transfer Engineering, 7,* 1-2, 1986, pp. 46-62.

9. R. Pernica and J. Cizek, "General Correlation for Prediction of Critical Heat Flux Ratio," *Proceedings of the 7th International Meeting on Nuclear Reactor Thermal-*

Hydraulics, NURETH-7, Saratoga Springs, NY, September 10 - 15, 1995, NUREG/CP-0142, Vol. 4.

10. R. Pernica and J. Cizek, *PG General Correlation of CHFR and Statistical Evaluation Results,* NRI Report, UJV-10156-T, February 1994.

11. D. C. Groeneveld et al., "The 1995 look-up table for critical heat flux in tubes," *Nuclear Engineering and Design*, Vol. 163, 1996, pp. 1-23.

12. D. C. Groeneveld et al., "Lookup Tables for Predicting CHF and Film-Boiling Heat Transfer: Past, Present, and Future," *Nuclear Technology*, Vol. 152, 2005, pp. 87-104.

13. D.C. Groeneveld, J.Q. Shan, A.Z. Vasić, L.K.H. Leung, A. Durmayaz, J. Yang, S.C. Cheng, and A. Tanase**, "**The 2006 CHF look-up table," *Nuclear Engineering and Design* 237 (2007) 1909-1922.

14. David D. Hall and Issam Mudawar, "Critical Heat Flux (CHF) for Water Flow in Tubes – I. Compilation and Assessment of World CHF Data," *International Journal of Heat and Mass Transfer*, Volume 43, 2000, pp. 2573-2604.

15. David D. Hall and Issam Mudawar, "Critical Heat Flux (CHF) for Water Flow in Tubes – II. Subcooled CHF Correlations," *International Journal of Heat and Mass Transfer*, Volume 43, 2000, pp. 2605-2640.

16. David D. Hall and Issam Mudawar, "Evaluation of Subcooled Critical Heat Flux Correlations Using the PU-BTPFL CHF Database for Vertical Upflow of Water in a Uniformly Heated Round Tube," *Nuclear Technology*, Vol. 117, pp. 234-247, Feb. 1997.

17. "Columbia University Data Books," Vol. 1 through 6 (January 1956).

18. D. C. Groeneveld, J. Q. Shan, A. Z. Vasi, L. K. H. Leung, A. Durmayaz, J. Yang, S. C. Cheng, and A. Tanase, "The 2005 CHF Look-Up Table," *The 11th International Topical Meeting on Nuclear Reactor Thermal-Hydraulics (NURETH-11)*, Paper: 166, Popes' Palace Conference Center, Avignon, France, October 2-6, 2005.

19. E. E. Feldman, "Fundamental Approach to TRIGA Steady-State Thermal-Hydraulic CHF Analysis," Presented at the 2007 International Meeting on Reduced Enrichment for Research and Test Reactors, September 23-27, 2007, Prague, Czech Republic and at the National Organization of Test, Research, and Training Reactors (TRTR) Meeting, September 17-20, 2007, Lincoln City, Oregon.

20. R. T. Jensen and D. L. Newell, "Thermal Hydraulic Calculations to Support Increase in Operation Power in McClellen Nuclear Radiation Center (MNRC) TRIGA Reactor," 1998 RELAP5 International User's Seminar, May 17-22, 1998.

21. D. V. Rao and M. S. El-Genk, *Critical Heat Flux Predictions for the Sandia Annular Core Research Reactor*, Sand90-7089, Institute for Space and Nuclear Power Studies, University of New Mexico, Albuquerque, NM 87131, August 1994.

22. Mohamed S. El-Genk, Stanley J. Haynes, and Sung-Ho Kim, "Experimental Studies of Critical Heat Flux for Low Flow of Water in Vertical Annuli at Near Atmospheric Pressure," *International Journal of Heat and Mass Transfer*, Volume 31, No. 11, 1988, pp. 2291-2304.

23. W. L. Whittemore and G. B. West, *Summary of Power Stability Tests (Chugging) for a Hexagonal TRIGA Reactor Core*, General Atomics report TOO-9, August 1996.

24. W. L. Whittemore, *Power Stability Tests at the McClellan Nuclear Radiation Center 2 MW TRIGA Reactor*, General Atomics report TOO-10, April 1997.

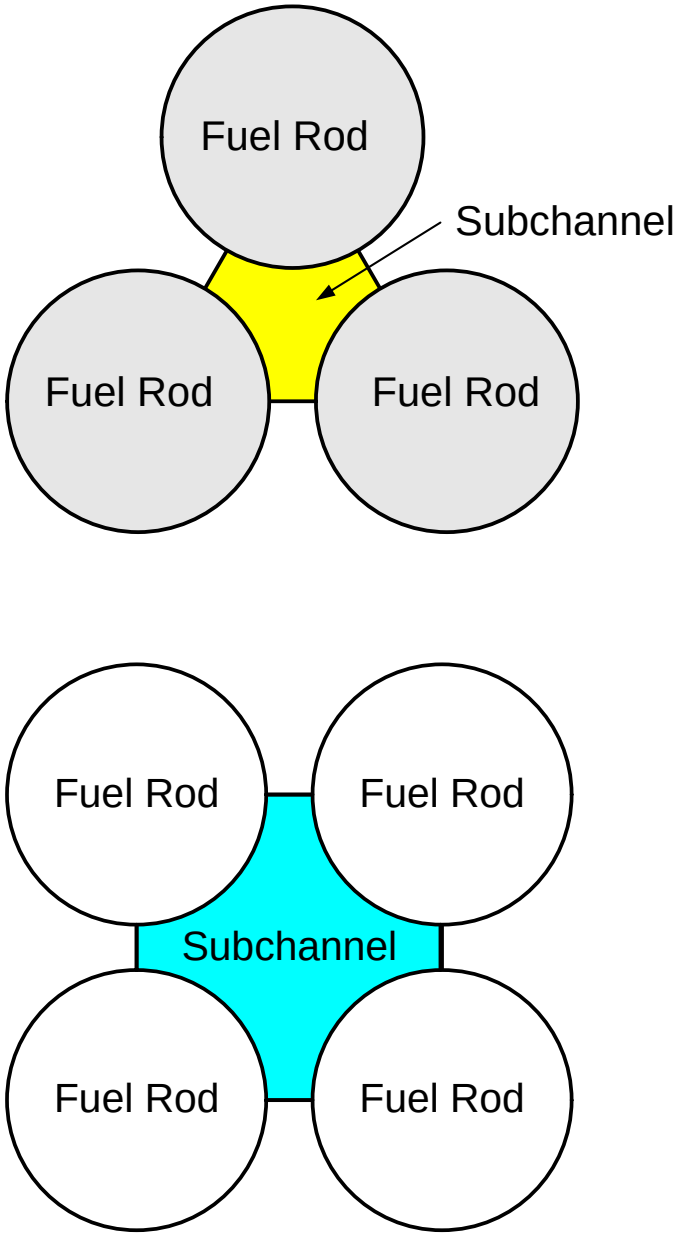

Figure 1. Example TRIGA Coolant Subchannels Used in Modeling

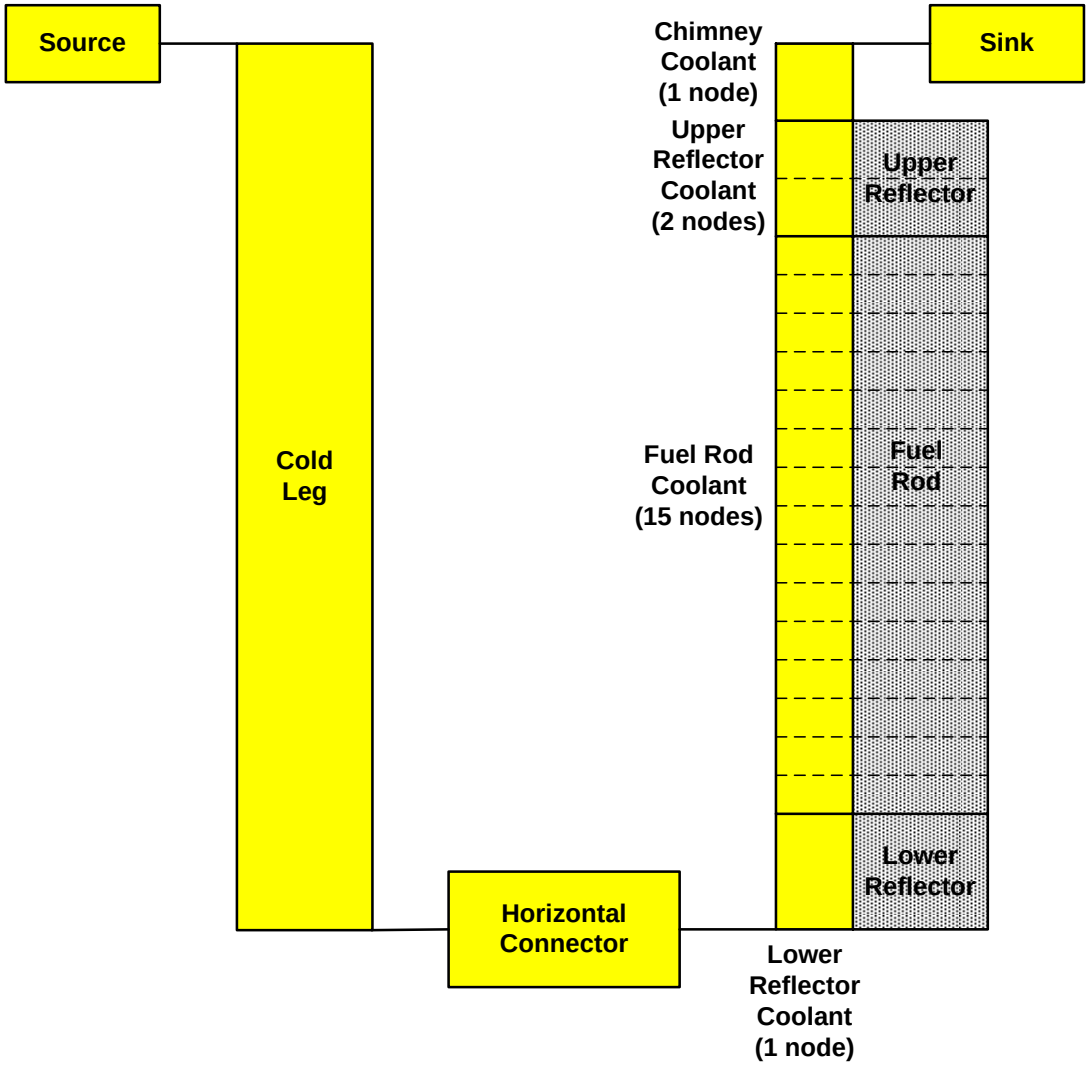

Figure 2. Schematic View of RELAP5-3D Model of TRIGA Coolant Channel

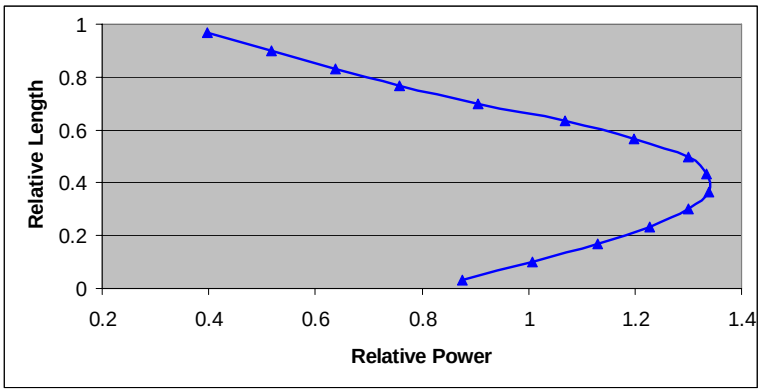

Figure 3. Axial Power Shape for the Hottest Channel of the Hexagonal Pitch TRIGA Reactor

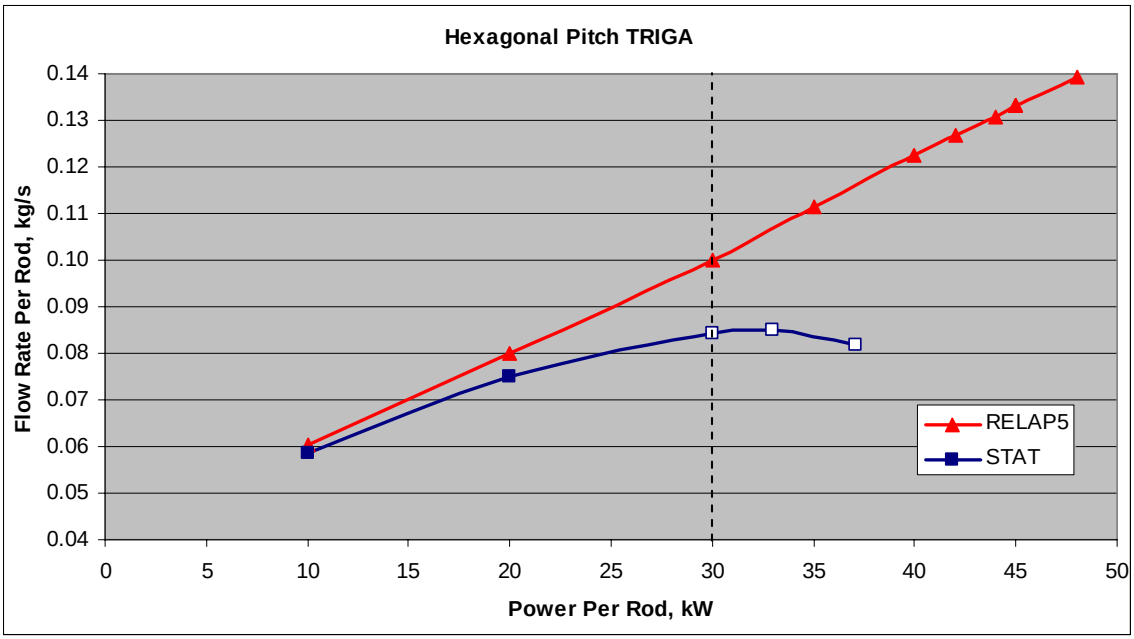

Figure 4. Comparison of the STAT and RELAP5-3D Flow Rates for the Hexagonal Pitch TRIGA Reactor

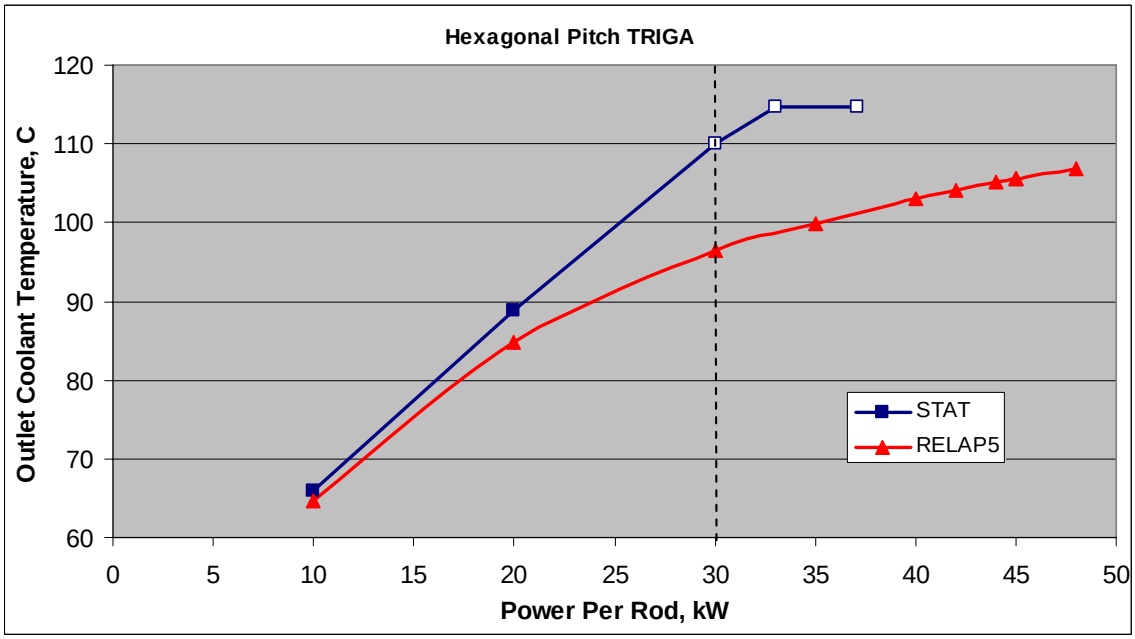

Figure 5. Comparison of the STAT and RELAP5-3D Outlet Coolant Temperatures for the Hexagonal Pitch TRIGA Reactor

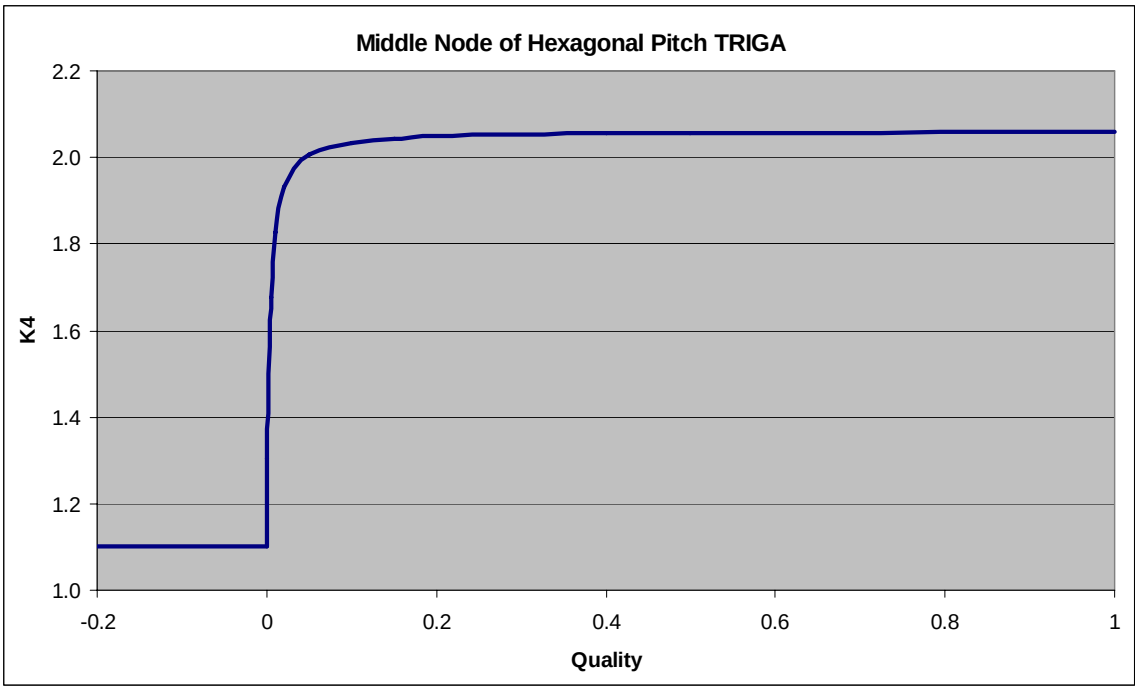

Figure 6. K_4 for Middle Axial Node of Hexagonal Pitch TRIGA Reactor

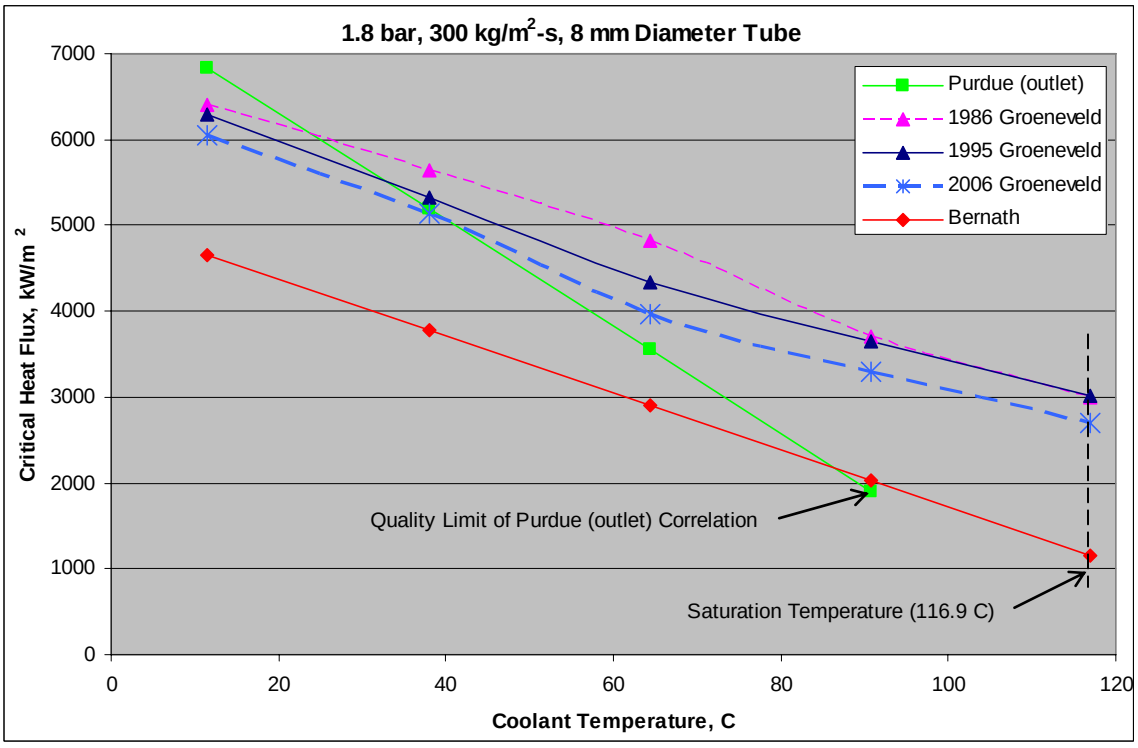

Figure 7. CHF vs. Temperature for an 8 mm Diameter Tube

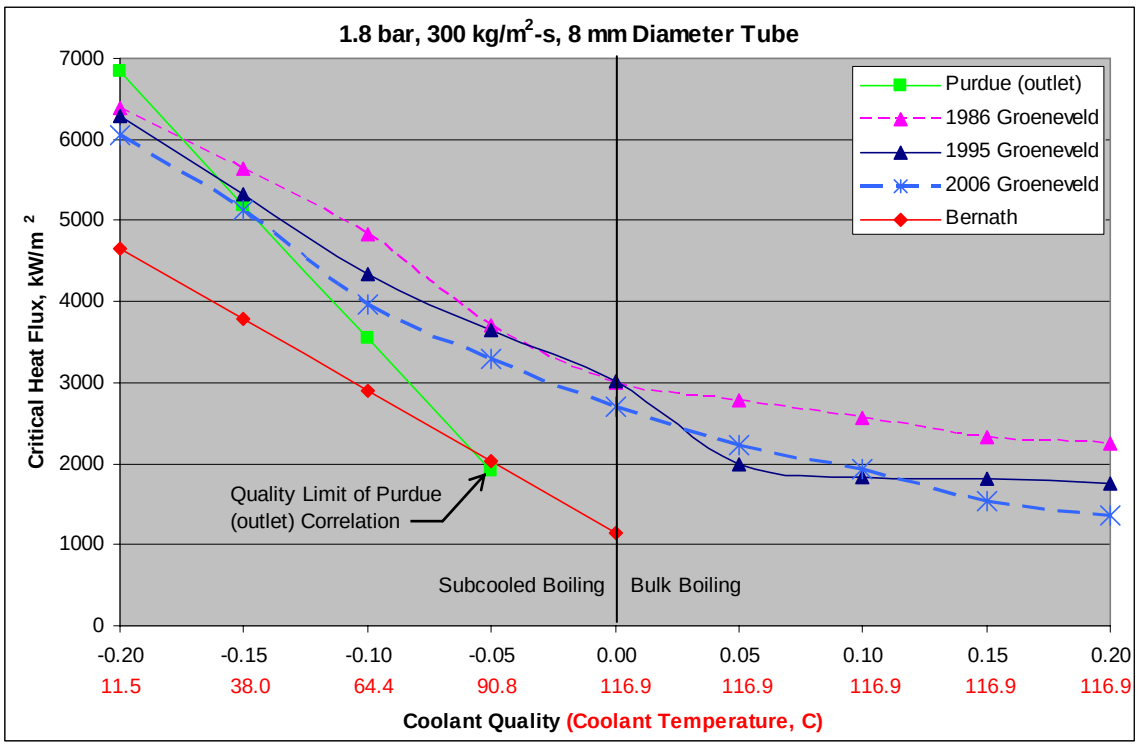

Figure 8. CHF vs. Quality for an 8 mm Diameter Tube

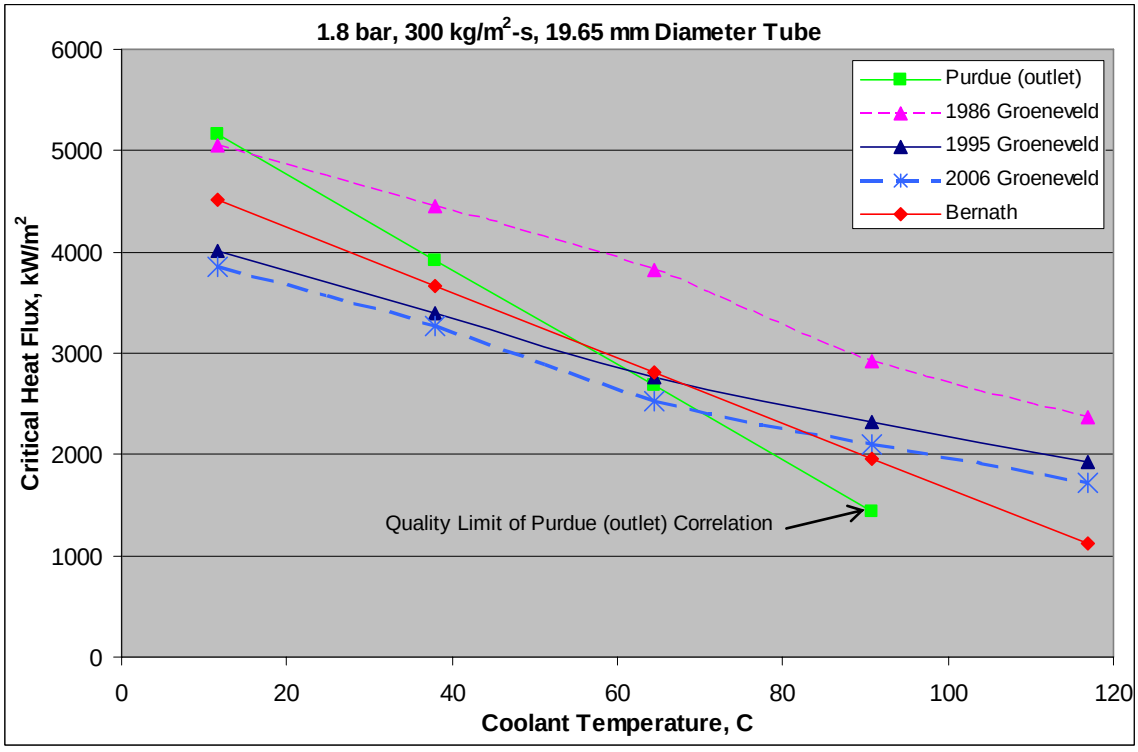

Figure 9. CHF vs. Temperature for a 19.65 mm Diameter Tube

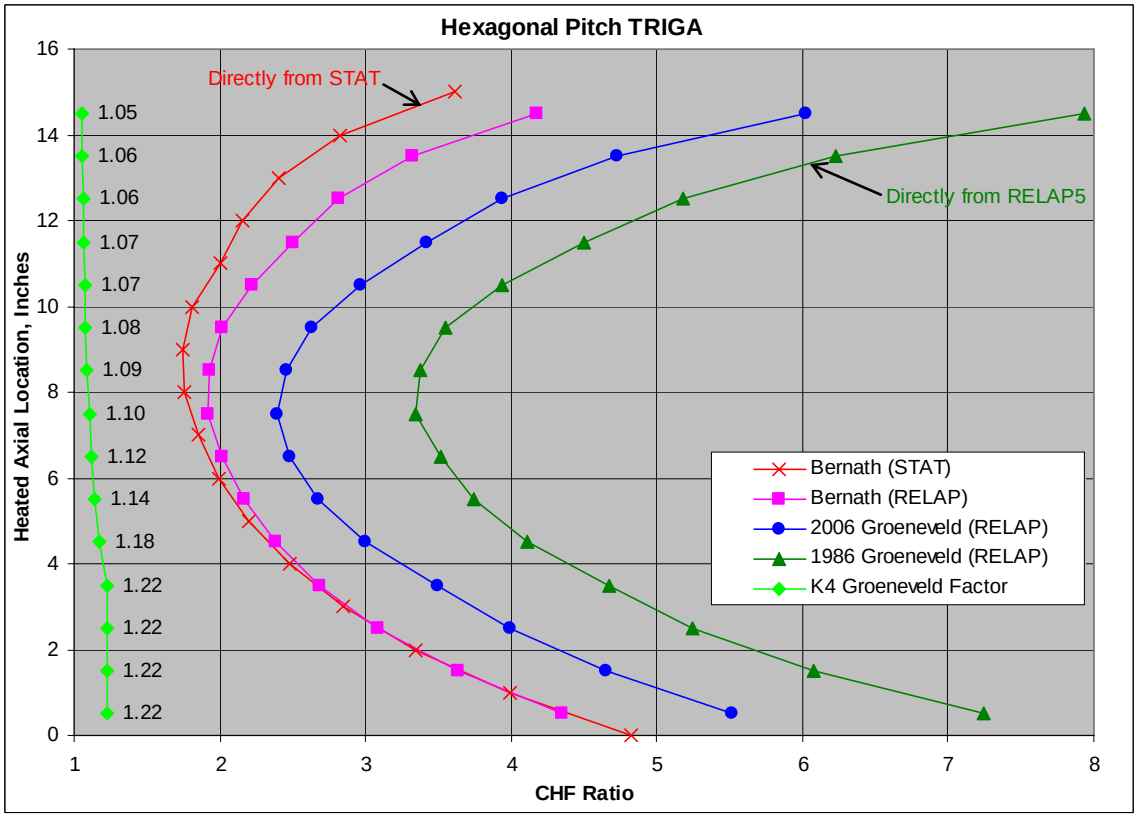

Figure 10. CHF Ratios for the Hexagonal Pitch TRIGA Evaluated at Nominal Power, where the Highest Power Rod is 30 kW

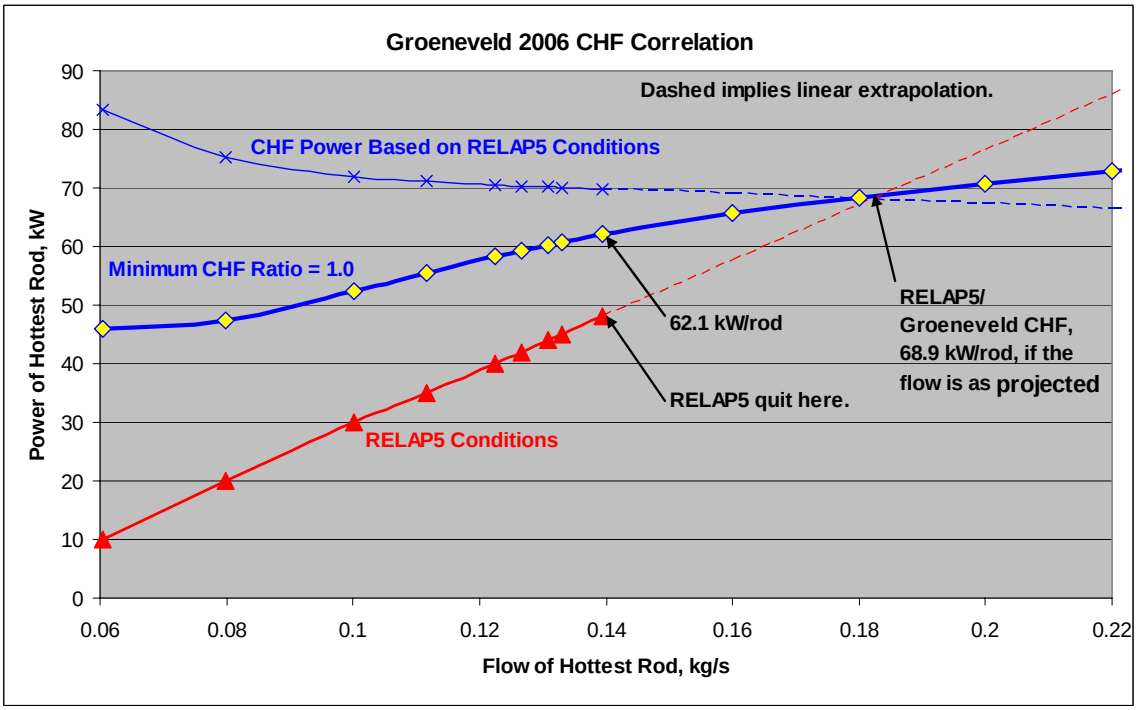

Figure 11. CHF Power of the Hexagonal Pitch TRIGA Reactor Based on the Groeneveld 2006 Table

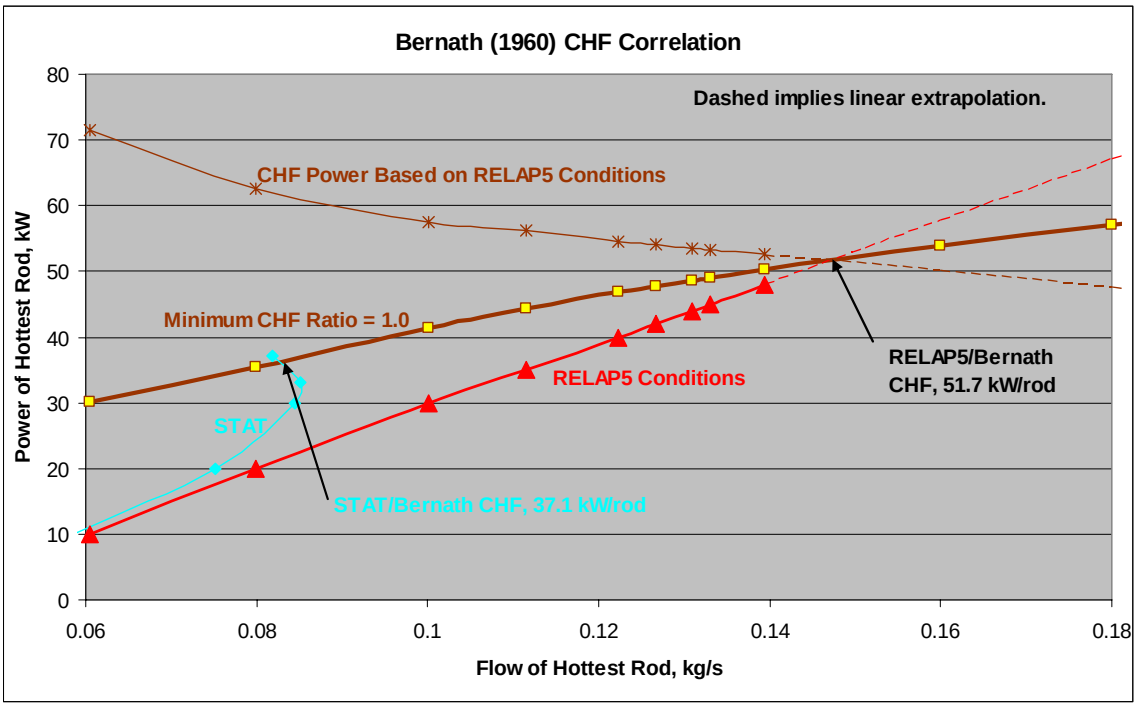

Figure 12. CHF Power of the Hexagonal Pitch TRIGA Reactor Based on the Bernath Correlation

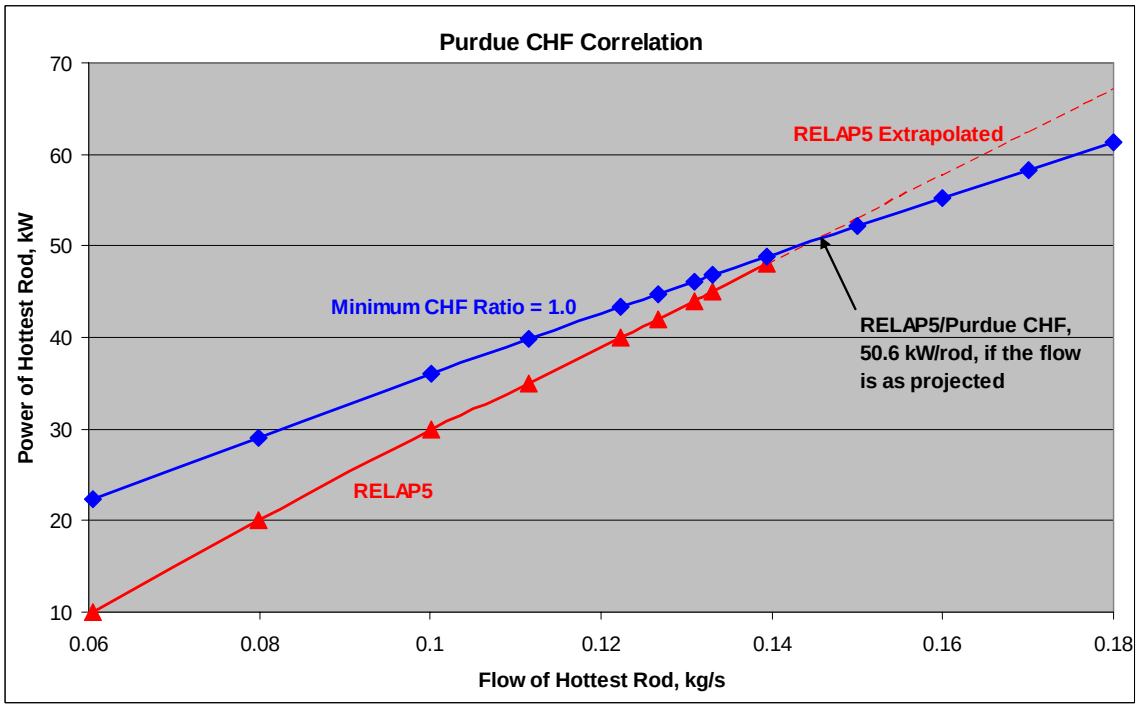

Figure 13. CHF Power of the Hexagonal Pitch TRIGA Reactor Based on the Purdue (Outlet) Correlation

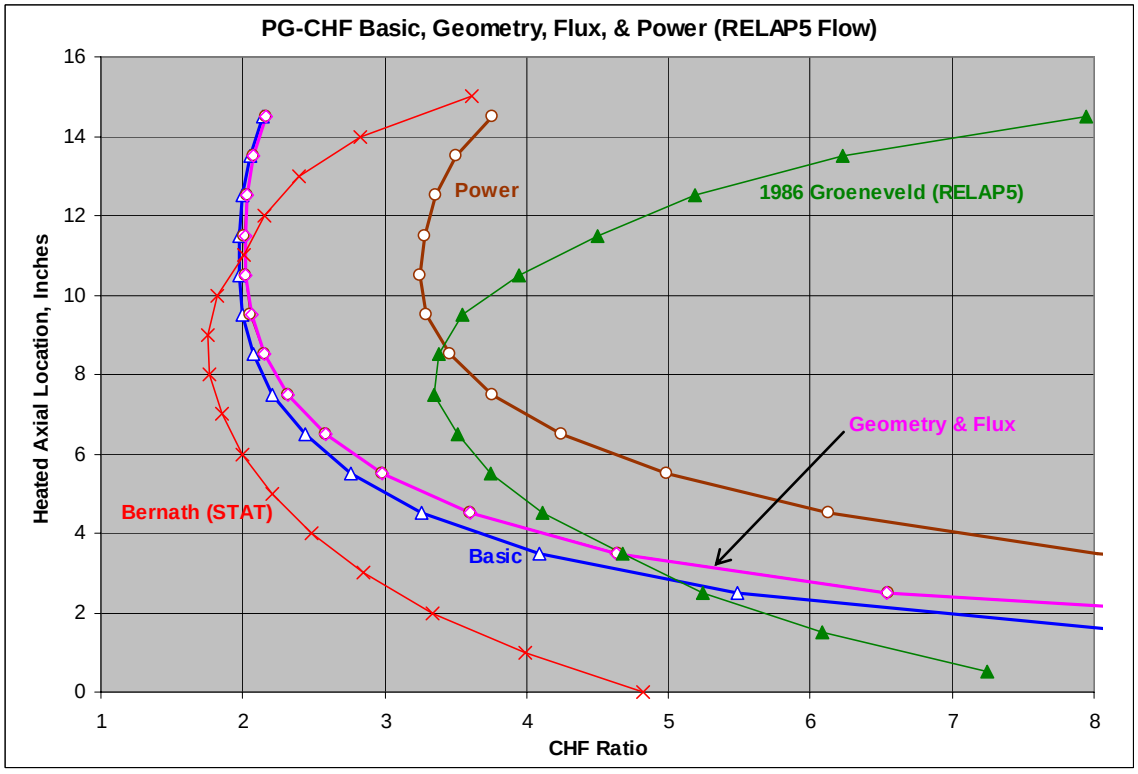

Figure 14. PG-CHF CHF Ratios for the Hexagonal Pitch TRIGA Evaluated at Nominal Power, where the Highest Power Rod is 30 kW

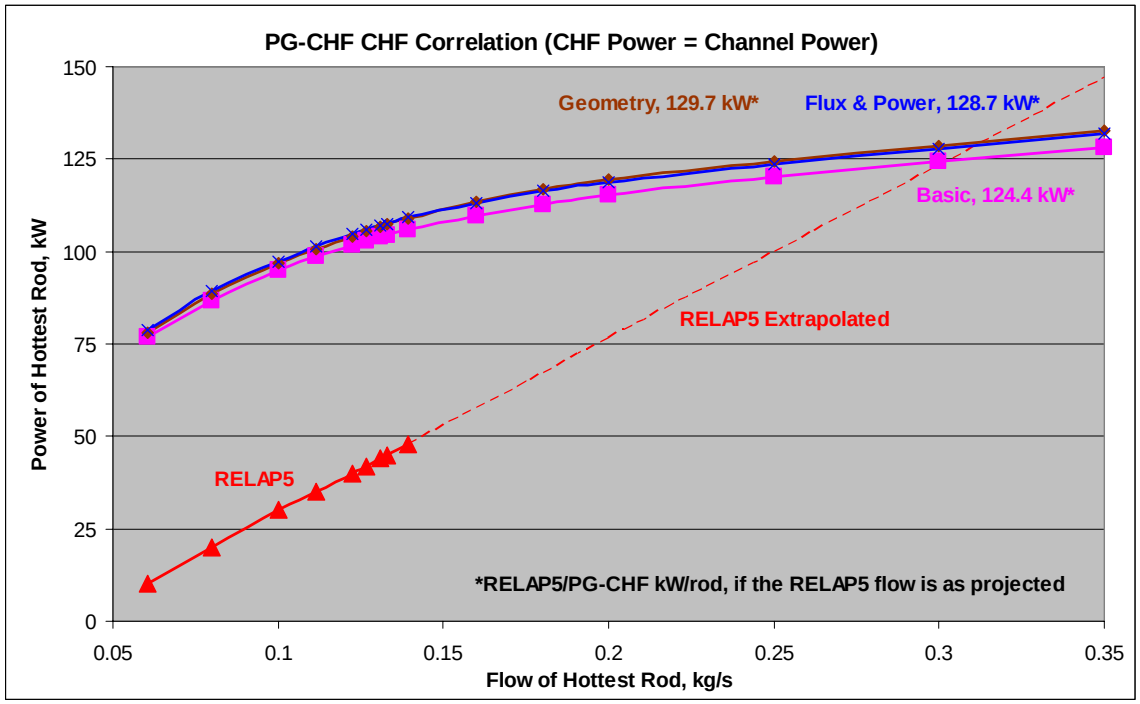

Figure 15. CHF Power of the Hexagonal Pitch TRIGA Reactor Based on the PG-CHF Rod Bundle Correlations

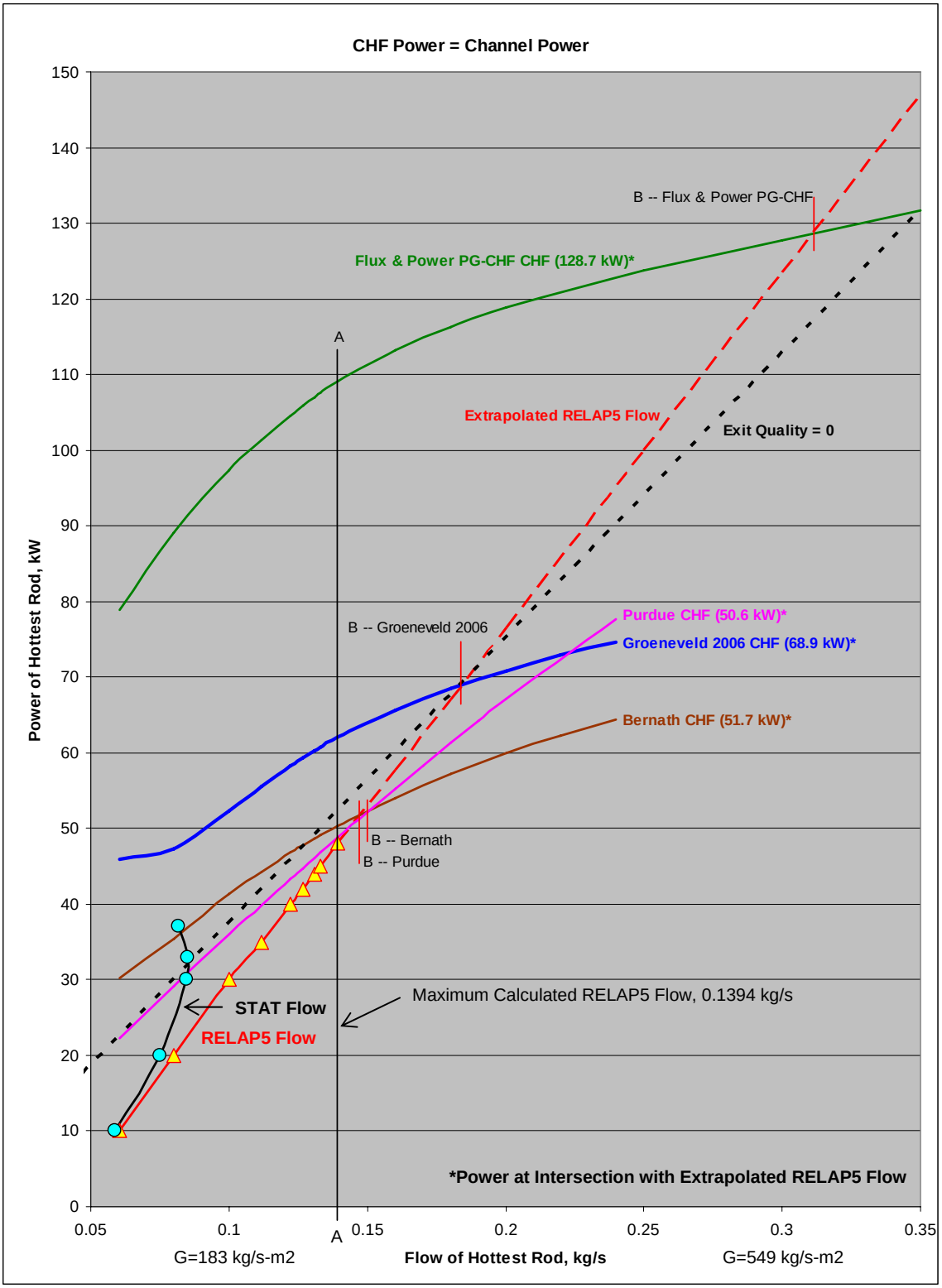

Figure 16. Comparison of the CHF Predictions for the Hexagonal Pitch TRIGA Reactor

Table 1. TRIGA Generic Reactor Parameters

	Reactor	
Parameter	**Hexagonal Pitch**	**Rectangular Pitch**
Fuel element pitch	Hexagonal	Rectangular conversion
Flow area per rod, cm^2	5.464	5.532
Hydraulic diameter, mm	18.64	19.65
Rod (heated) diameter, mm	37.34	35.84
Inlet temperature, C (F)	25 (77)	30 (86)
Pressure (~mid-core), bars	1.68	1.80
Saturation temperature, C (F)	114.8 (238.6)	116.9 (242.4)
Inlet K-loss	3.58	1.672
Exit K-loss	3.0	0.6
Reactor power, MW	2.0	1.0
Number of rods	100	90
Radial power factor (hot. rod)	1.5	1.565
Power of hottest rod, kW	30.0	17.4

Table 2. CHF Power of the Rectangular Pitch TRIGA Based on the STAT Code

VDF	Reactor Power, MW
0.	2.21
0.3	2.42
1.0	2.81

Table 3. Representative TRIGA Reactor Conditions

	Nominal Conditions	CHF Conditions
Mixed-mean coolant temperature	Below boiling (subcooled)	Below or possibly at boiling (subcooled or possibly saturated)
Mass flux, kg/m^2-s	~100	~300
Velocity, ft/s	~1/3	~1
Pressure, bar	~1.8	~1.8

Table 4. Summary of CHF Results for Hexagonal Pitch TRIGA Reactor

Flow	CHF Correlation	Rod CHF Power, kW			CHF Ratio*		
		A**	B+	C++	A**	B+	C++
STAT	Bernath		37.1	52.5		1.24	1.75
RELAP5	Bernath	50.3	51.7	57.5	1.65	1.69	1.92
	Purdue	48.9	50.6		1.63	1.69	
	Groeneveld 2006	62.1	68.9	71.9	2.07	2.30	2.40
	Groeneveld 1986			100.3			3.30
	PG-CHF, Basic	105.9	124.4		3.53	4.15	
	PG-CHF, Geometry	108.9	129.7		3.63	4.32	
	PG-CHF, Power or Flux	109.2	128.7		3.64	4.29	

*1.0 corresponds to 30 kW for the highest power rod and 2.0 MW for the reactor.
**A (RELAP5-3D Flow): CHF curve at maximum calculated flow per rod (0.1394 kg/s, thin vertical black line A-A in Figure 16), where RELAP5 flow begins to oscillate.
+B (Extrapolated RELAP5-3D Flow): Intersection of a CHF correlation curve and a reactor flow curve, as shown in Figure 16.
++C (Not Recommended): CHF based on calculated reactor power and flow at 30 kW/rod.

APPENDIX A – A BRIEF DESCRIPTION OF COOLANT QUALITY

Since quality is a key independent variable used in the Groeneveld tables and in other CHF correlations, a brief explanation may be helpful. Only the mixed-mean quality is used in the Groeneveld tables. It can be obtained by assuming that at any point of interest along the fluid steam the coolant is well-mixed. In the current context, quality, enthalpy (which can be thought of as a substitute for energy), and temperature are assumed to correspond to the well-mixed condition. Thus, at a location along the coolant stream where subcooled boiling is occurring, both liquid and vapor can be present together, but for the mixed-mean condition at that location, the temperature will always be below the saturation temperature as if there is no vapor present. The quality at location 1 along the channel, X_1, is given by $X_1 = (h_1 - h_f) / (h_g - h_f)$, where h is the enthalpy per unit mass (or specific enthalpy). The subscript 1 corresponds to location 1 along the channel. The subscripts f and g correspond to saturated liquid and vapor, respectively. $h_g - h_f$ is the heat of vaporization. A quality of 0 implies $h_1=h_f$, a saturated liquid condition in which there is no vapor present. A quality of 1.0 implies $h_1=h_g$, a saturated vapor condition in which there is no liquid present. A quality of 0.15 implies that the enthalpy per unit mass is 15% of the way from all-liquid to all-vapor. For this condition 15% of the well-mixed mass will be vapor and 85% will be liquid. The temperature for all qualities between 0 and 1 is the saturation temperature. The above definition of quality also includes negative values of quality. These correspond to coolant temperatures below the saturation temperature. The above relationship for X_1 can be solved for h_1 to obtain $h_1 = h_f + X_1 (h_g - h_f)$. Thus, a quality of −0.15 implies a specific enthalpy that is 15% of the heat of vaporization less than that of the specific enthalpy of saturated liquid.

APPENDIX B – CHF PREDICTIONS FOR THE HIGHEST POWER ROD OF EACH OF FOUR TRIGA REACTORS

Each TRIGA reactor should be analyzed separately to predict the power at which CHF occurs. However, it is useful to compare the rod power at which CHF occurs in the various types of TRIGA reactors. There are differences among the reactors, such as water depth, inlet temperature, rod pitch, and inlet and outlet hydraulic resistances. This comparison is not intended or expected to be a replacement for performing a separate detailed CHF analysis for each reactor.

The author of Reference 1 has provided RELAP5/MOD3.2 channel flow rate versus power data for the Washington State University (WSU), the Texas A & M University (TAMU), the U. C. Davis McClellan Nuclear Radiation Center (MNRC), and Oregon State University (OSU) TRIGA reactors. WSU and TAMU have rectangular pitches, MNRC has a hexagonal pitch grid plate, and OSU has a circular one. In the calculations, each of the reactors was assumed to have an inlet temperature of 30° C. In each case a channel adjacent to the rod with the highest power was used. This analysis is not intended to challenge or supersede the existing safety analyses for any of the four reactors considered. Some of the details of the RELAP5/MOD3.2 analysis, such as the calculation of inlet and outlet hydraulic form loses, can be found in Reference 1.

The author of Reference 1 provided the RELAP5/MOD3.2 computer input and output listings rather than a table of RELAP5/MOD3.2 results. Thus, any errors in interpreting the data belong to the current author. The methods outlined in the current report were used to generate Figures B-1 through B-4. Since the computer outputs did not include flow rate as a function of time, an indirect method was used to detect the presence of flow oscillations. It has been observed that when flow oscillations are present, at the end of the final time interval the solution contains an axial variation of flow along the length of channel. This variation was used to infer the presence of flow oscillations.

In each set of RELAP5/MOD3.2 results the highest power case had an indication of a flow oscillation. This power level is identified in Figures B-1 through B-3 by a white-filled symbol on the RELAP5/MOD3.2 curve. For each of these three figures, a linear curve fit of all of the non-oscillatory points was used to produce the extrapolation indicated by the thin red dashed line. This approach was not used in Figure B-4, however, due to an obvious change in slope near the end of the RELAP5 curve. This change in slope caused the current author to use the RELAP5/MOD3.2 model provided by Reference 1 to run several new cases with Version 2.3 of the RELAP5-3D code, as indicated by the four yellow-filled symbols in Figure B-4. For these four cases, whose rod powers are 53.3, 57.8, 62.2, and 66.7 kW, the pseudo-transient solution was extended by 1000 s to 4000 s and flow was printed and plotted as a function of time. Only the 62.2 kW power level was included in the original RELAP5/MOD3.2 data. The RELAP5-3D flow rate prediction for this power level is only 0.4% less than its RELAP5/MOD3.2 counterpart. Thus, the two results essentially agree. The rod power that indicated a flow oscillation is 71.1 kW, which is only 6.7% greater than the final 66.7 kW value in Figure

B-4 of. The 71.1 kW case was also rerun with the RELAP5-3D code. The pseudo-transient solution was extended and smaller time steps were used. The solution showed a large flow oscillation, which could not be approximated by a single power-versus-flow point in Figure B-4.

As Figures B-2 (TAMU) and B-3 (OSU) show, a large flow extrapolation of the RELAP5/MOD3.2 curve is sometimes needed to intersect the 2006 Groeneveld CHF curve. A linear curve-fit extrapolation may be too optimistic. It is likely that as the power is increased the rapid increase in vapor will cause the hydraulic resistance to increase faster than the buoyancy. This would tend to cause the RELAP5/MOD3.2 curve to bend upward, as demonstrated by the RELAP5 curve in Figure B-4 (MNRC). Thus, it is strongly recommended that extrapolated flow data not be used for CHF analysis.

The CHF predictions for the four reactors are summarized in Table B-1. Two 2006 Groeneveld solutions are provided. Method A, which provides lower values of CHF power, evaluates the 2006 Groeneveld curve at the highest non-oscillatory flow calculated by RELAP5 and is the recommended method. Method B, which is not recommended, uses the extrapolated RELAP5/MOD3.2 flow curves of Figures B-1 through B-3 and a linear extrapolation based on the last two flows of Figure B-4.

As explained in Section 3.5, the rapid increase in the K_4 Groeneveld factor as the quality becomes positive can cause there to be three power solutions in which the minimum CHF ratio is 1.0. At each flow rate where this occurs, the minimum of the three 2006 Groeneveld CHF powers must be selected and plotted on the CHF curve. This behavior of the K_4 factor is the reason for the sudden decrease at the left ends of the 2006 Groeneveld curves in Figures B-1 through B-4. Otherwise these curves would have increased monotonically.

Figure B-5 compares the four RELAP5 flow curves, the four 2006 Groeneveld CHF curves, and the four Bernath CHF curves for the four reactors. A different color is used to represent each reactor. The solid curves are RELAP5 flow curves without extrapolation, but including the oscillatory point at the maximum power for WSU, TAMU, and OSU. (The MNRC RELAP5 curve for increased K-losses is discussed below.) The large dashed lines form the 2006 Groeneveld CHF curves. The short dashed lines form the Bernath CHF curves.

The RELAP5 curves in Figure B-5 show that MNRC has considerably more flow for a given power level than do any of the other three reactors. This is to be expected, at least in part, because, as shown in Table B-2, the inlet and out form- (or K-) losses for MNRC tend to be much smaller than those of the other three reactors. The effect of these K-losses on the MNRC reactor was investigated by the current author by using the Reference 1 RELAP5 model for MNRC with the inlet and the outlet K-losses each increased to 1.50. The resultant MNRC RELAP5 curve, Figure B-5, is very close to the RELAP5 curves for the other three reactors.

As Table B-1 shows, when the MNRC inlet and outlet K-losses are each increased to 1.5, there are substantial hydraulic similarities – as represented by hydraulic diameter, flow area, and total K-loss – among the WSU, TAMU, and MNRC reactors. Thus, the very close proximity of the MNRC curve for the increased K-losses to the solid WSU and TAMU curves is to be expected. In addition, these three curves and the solid OSU curve do not show a sudden increase in slope. The sudden change in slope exhibited by the normal MNRC curve may be due to its very low K-losses. As the power is increased, subcooled nucleate boiling begins and generates voids. The voids increase in volume as the power is increased and cause the frictional resistance and the buoyancy along the length of the rod to increase as the void volume increases. The effectiveness of this increased resistance in impeding the increase in flow caused by the increase in buoyancy is larger when the K-losses are small.

Since K-loss is a difficult quantity to accurately determine, it is important to assess the sensitivity of CHF to the K-loss values used in the analysis. The two sets of MNRC results in Table B-1 are intended to directly address this point. As discussed with regard to Figure B-5, the substantial increase in MNRC K-losses substantially reduces rod flow rates. Figure B-5 also shows that the Bernath and 2006 Groeneveld CHF curves are only moderately sensitive to flow. Thus, a large reduction in flow corresponds to only a small reduction in CHF power. The MNRC results in Table B-1 show that a more than 2.5 fold increase in K-losses (from 0.58 or 0.59 to 1.50) reduces CHF power predicted by the 2006 Groeneveld correlation by 3.1 % (from 70.5 to 68.3 kW) and the CHF power predicted by the Bernath correlation by 2.1 % (from 56.6 to 55.3 kW).

The OSU Groeneveld CHF power curve in Figure B-5 is above the other three, the OSU Bernath CHF curve is below the other three, and the OSU RELAP5 curve of power versus flow is above the other RELAP5 curves. The relative position of the OSU RELAP5 curve is largely due to greater hydraulic resistance for the OSU rod channel considered. This is a result of OSU's smaller hydraulic diameter and flow area, as indicated in Table B-1. The smaller hydraulic diameter contributes to a larger value of 2006 Groeneveld CHF power because this CHF power is proportional to its multiplicative K_1 factor, which in turn is inversely proportional to the square root of hydraulic diameter. The hydraulic diameter can have the opposite effect on the Bernath CHF power in that decreasing the hydraulic diameter can decrease the Bernath CHF power.

As shown in Table B-1, MNRC has the largest 2006 Groeneveld CHF power, 70.5 kW per rod, using Method A. The values for the other three reactors are close together. The value for MNRC is only 15.2 % greater than the smallest value, 61.2 kW. The Bernath CHF results show a larger variation, with the largest value, 56.5 kW per rod for MNRC, 41.6% larger than the smallest value, 40.4 kW.

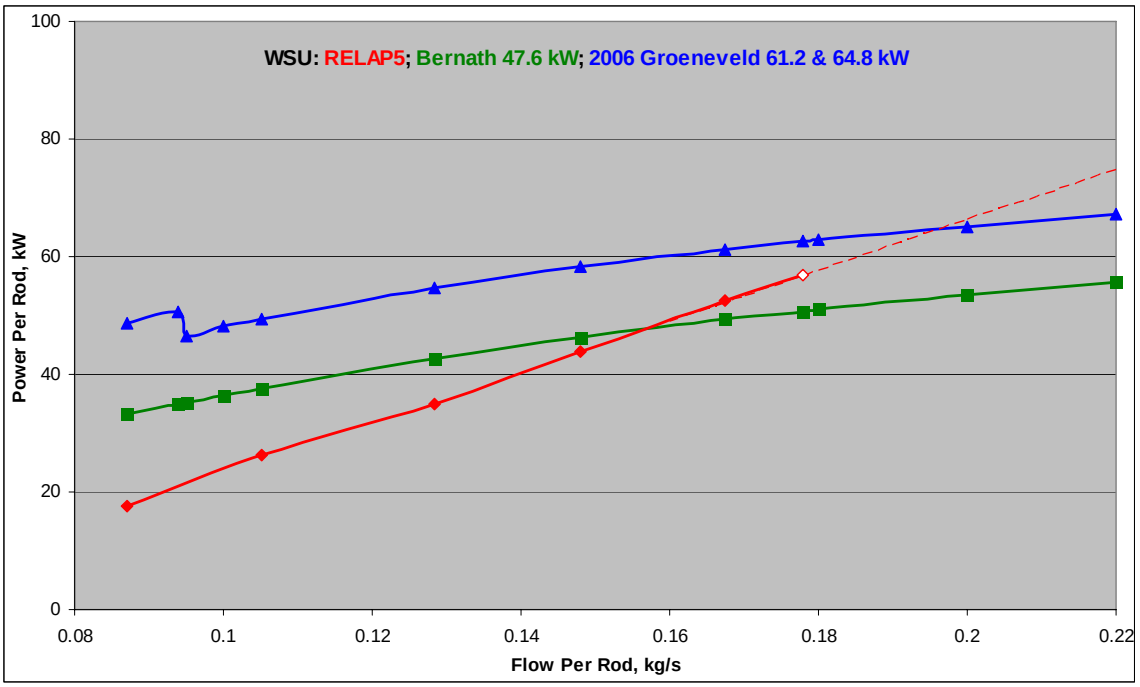

Figure B-1. Power versus Flow for the Highest Power Rod in the WSU TRIGA Reactor

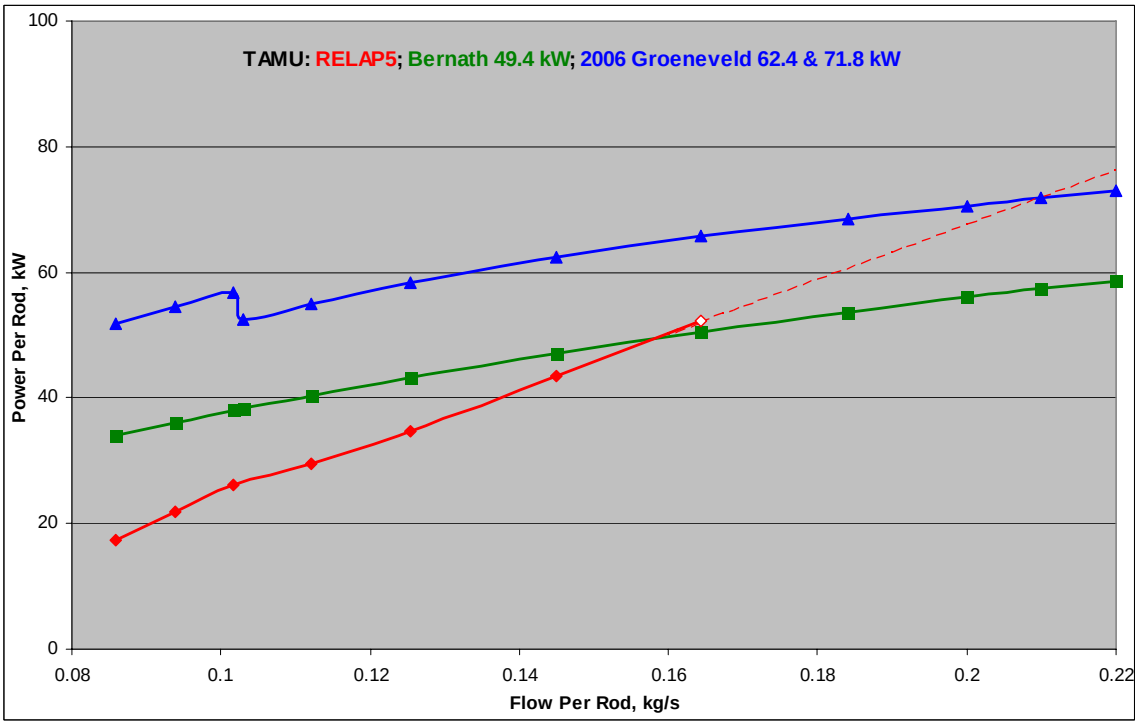

Figure B-2. Power versus Flow for the Highest Power Rod in the TAMU TRIGA Reactor

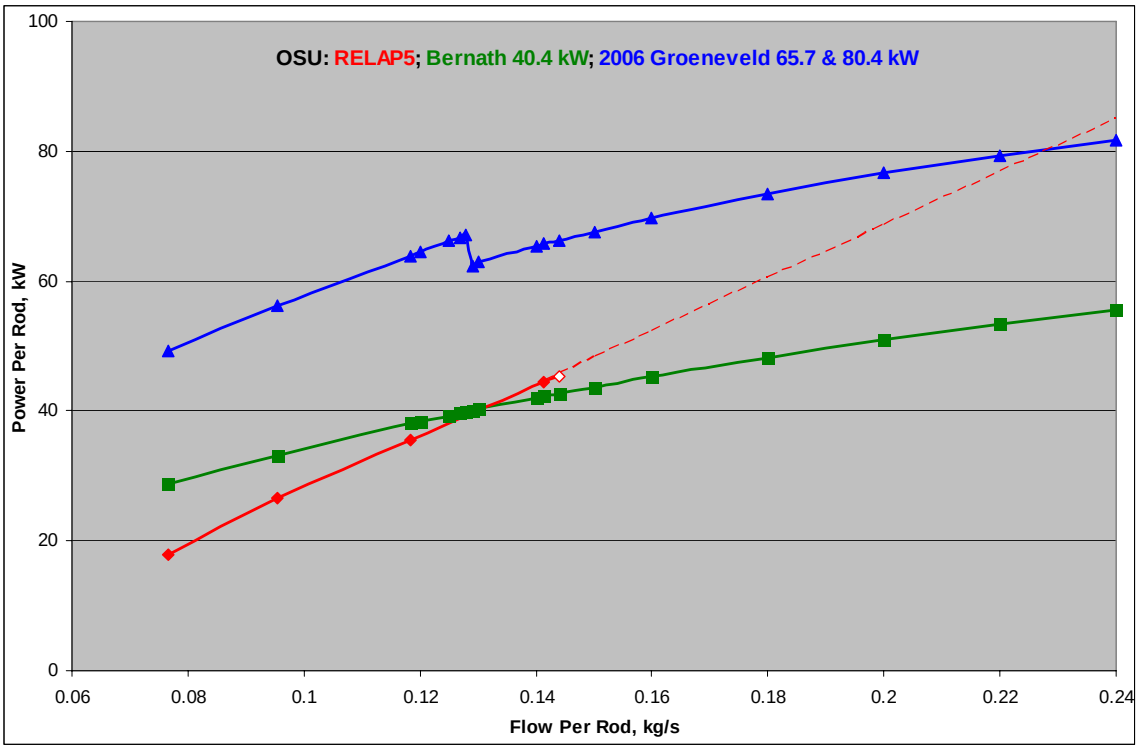

Figure B-3. Power versus Flow for the Highest Power Rod in the OSU TRIGA Reactor

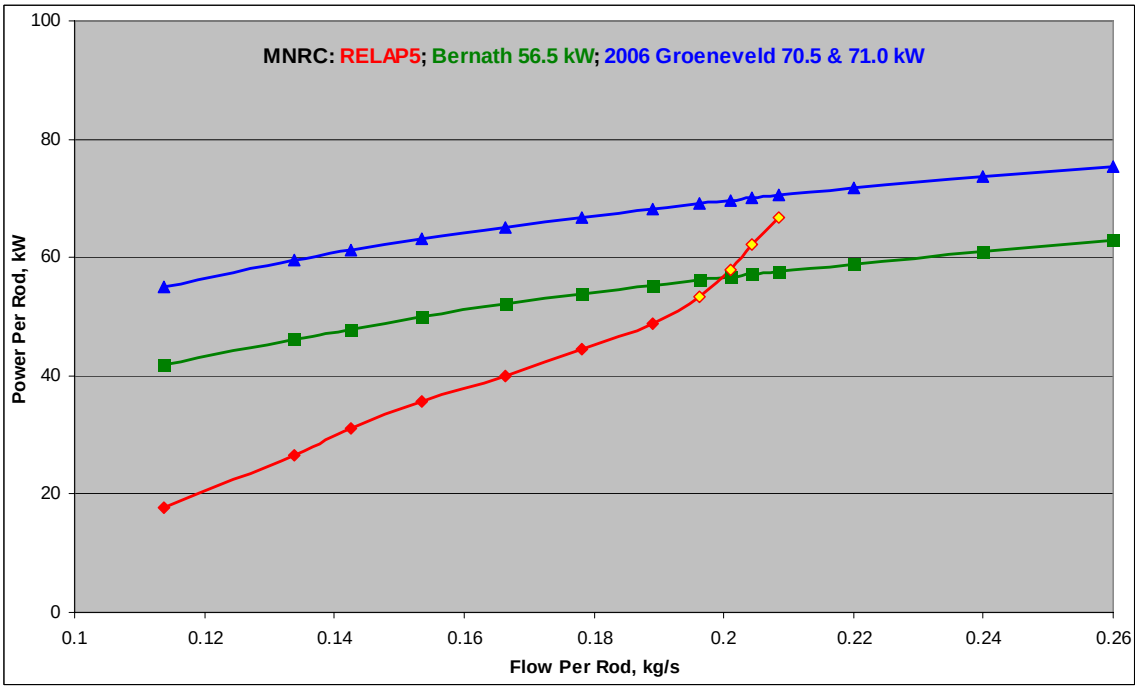

Figure B-4. Power versus Flow for the Highest Power Rod in the MNRC TRIGA Reactor

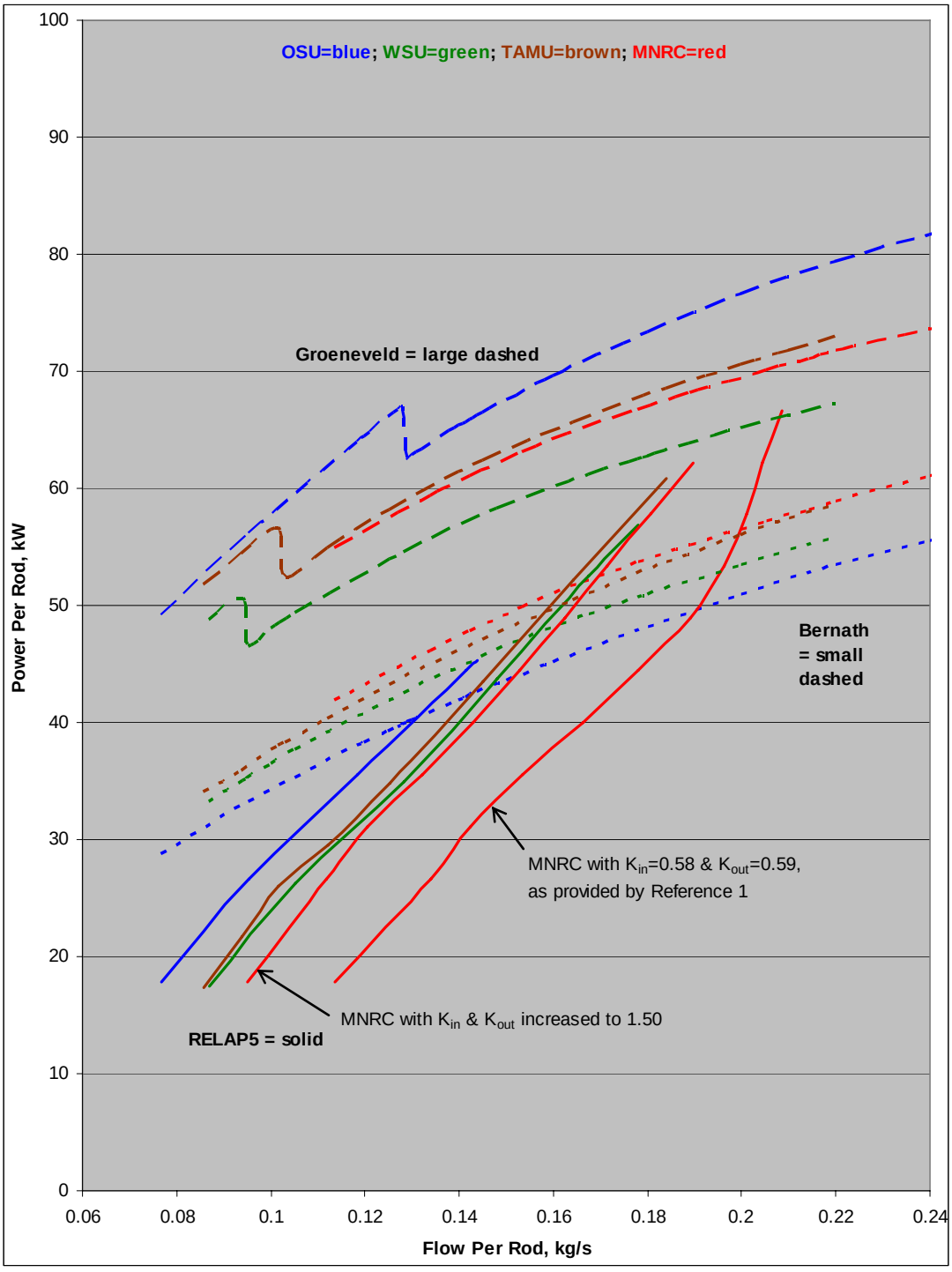

Figure B-5. Summary of RELAP5, 2006 Groeneveld, and Bernath Results for Four Reactors

Table B-1. Summary of CHF Results and Hydraulic Parameters

Reactor	Bernath CHF, kW	2006 Groeneveld CHF, kW		Hydraulic Diameter, mm	Flow Area per Rod, cm^2	K-losses		
		Method A	Method B			Inlet	Outlet	Total
WSU	47.6	61.2	64.8	17.816	5.0149	2.02	1.38	3.40
TAMU	49.4	62.4	71.8	16.938	4.7678	1.72	1.30	3.02
OSU	40.4	65.7	80.4	13.890	4.0868	2.26	0.63	2.89
MNRC*	56.5	70.5	71.0**	18.318	5.3902	0.58	0.59	1.17
	55.3	68.3				1.50	1.50	3.00

***The Reference 1 inlet and outlet K-losses for MNRC are 0.58 and 0.59, respectively. The 1.50 values were analyzed to assess the sensitivity of the MNRC flow and CHF solutions to the K-loss values.**

****As explained in the text, due to a sharp change in slope, the RELAP5-3D flow extrapolation for MNRC is based on only the two highest non-oscillatory flow values.**

Nuclear Engineering Division
Argonne National Laboratory
9700 South Cass Avenue, Bldg. 208
Argonne, IL 60439-4842

www.anl.gov

UChicago ▶ Argonne LLC

A U.S. Department of Energy laboratory
managed by UChicago Argonne, LLC